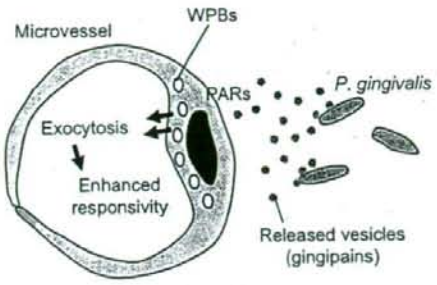

Fig. 5. Schematic of the effect of vesicle-associated RgpA on vascular endothelial cells.

RgpA may activate PAR signaling, leading to activation and promotion of leukocyte adhesion to the vascular endothelium, which links inflammation and coagulation in a variety of pathological settings.

P. gingivalis has a broad array of virulence factors as immunostimulatory compounds [21]. Several factors function as agonists for Toll-like receptor (TLR) 2 and TLR4 [22–25]. We found that IL-8 production not only by *P. gingivalis* LPS and HKPG but also by TLR4-agonistic *E. coli* LPS, TLR2-agonistic Pam_3CSK_4 and IL-1β was upregulated by RgpA, suggesting the synergism of TLRs/IL-1R and PARs. Indeed, several recent studies have suggested that TLRs and PARs synergistically function in induction of proinflammatory responses [26,27]. The presence of gingipains at the site of *P. gingivalis* infection may affect responsiveness of the vascular endothelium to virulence factors from *P. gingivalis*.

WPB exocytosis induces release of storage compounds and may control local or systemic physiological and pathological effects, including leukocyte rolling, thrombus formation, vascular inflammation and angiogenesis. Storage components of WPBs have various vasoregulatory activities. We demonstrated that Ang-2 could regulate endothelial response to *P. gingivalis* (Fig. 4C). Ang-2 has been identified as a functional antagonist of Ang-1. Ang-2 sensitizes endothelial cells to TNF-α, thereby acting as a switch of vascular responsiveness towards inflammatory stimuli [16]. It has been suggested that diabetes, an important risk factor for periodontal disease, induces increase in Ang-2 transcription and expression [28]. Thus, Ang-2 released from WPBs may be an important determinant of the severity of periodontal diseases caused by *P. gingivalis* infection.

Our study proposes that *P. gingivalis* infection can modulate inflammatory responses of vascular endothelial cells through release of gingipains (Fig. 5). Such an effect may have a crucial role in the initiation and regulation of periodontitis.

Acknowledgements

This work was supported by the Grant-in-Aid for Young Scientists (B):18791363 to T.I. and the AGU High-Tech Research Center Project to T.N. provided by the Ministry of Education, Culture, Sports, Science and Technology, Japan.

References

[1] R.J. Genco, Host responses in periodontal diseases: current
J. Periodontol. 63 (1992) 338–355.
[2] S.C. Holt, T.E. Bramanti, Factors in virulence expression and th
periodontal disease pathogenesis, Crit. Rev. Oral Biol. Med.
177–281.
[3] Z. Chen, J. Potempa, A. Polanowski, M. Wikstrom, J. Travis, P
and characterization of a 50-kDa cysteine proteinase (gingip
Porphyromonas gingivalis, J. Biol. Chem. 267 (1992) 18896–
[4] T. Kadowaki, M. Yoneda, K. Okamoto, K. Maeda, K. Yamamo
cation and characterization of a novel arginine-specific cystein
ase (argingipain) involved in the pathogenesis of periodont
from the culture supernatant of *Porphyromonas gingivalis*
Chem. 269 (1994) 21371–21378.
[5] R. Pike, W. McGraw, J. Potempa, J. Travis, Lysine- and arginin
proteinases from *Porphyromonas gingivalis*. Isolation, charac
and evidence for the existence of complexes with hema
J. Biol. Chem. 269 (1994) 406–411.
[6] T. Imamura, R.N. Pike, J. Potempa, J. Travis, Pathogenesis of
titis: a major arginine-specific cysteine proteinase from *Porph*
gingivalis induces vascular permeability enhancement through
of the kallikrein/kinin pathway, J. Clin. Invest. 94 (1994) 361
[7] T. Imamura, J. Potempa, R.N. Pike, J.N. Moore, M.H. Barton,
Effect of free and vesicle-bound cysteine proteinases of *Porph*
gingivalis on plasma clot formation: implications for bleeding
at periodontitis sites, Infect. Immun. 63 (1995) 4877–4882.
[8] T. Into, M. Inomata, Y. Kanno, T. Matsuyama, M. Mac
Y. Izumi, T. Imamura, M. Nakashima, T. Noguchi, K. Matsus
nine-specific gingipains from *Porphyromonas gingivalis* depri
tive functions of secretory leucocyte protease inhibitor in p
tissue, Clin. Exp. Immunol. 145 (2006) 545–554.
[9] T. Into, Y. Kanno, J.-I. Dohkan, M. Nakashima, M.
K.-I. Shibata, C.J. Lowenstein, K. Matsushita, Pathogen reco
toll-like receptor 2 activates Weibel-Palade body exocytosis
aortic endothelial cells, J. Biol. Chem. 282 (2007) 8134–814
[10] A. Uehara, K. Muramoto, T. Imamura, K. Nakayama, J.
J. Travis, S. Sugawara, H. Takada, Arginine-specific gingip
Porphyromonas gingivalis stimulate production of hepatocy
factor (scatter factor) through protease-activated receptors
gingival fibroblasts in culture, J. Immunol. 175 (2005) 6076–
[11] P.J. O'Brien, M. Molino, M. Kahn, L.F. Brass, Protease activ
tors: theme and variations, Oncogene 20 (2001) 1570–1581.
[12] S.R. Coughlin, Thrombin signalling and protease-activated
Nature 407 (2000) 258–264.
[13] C.J. Lowenstein, C.N. Morrell, M. Yamakuchi, Regulation
Palade body exocytosis, Trends Cardiovasc. Med. 15 (2005)
[14] M.G. Rondaij, R. Bierings, A. Kragt, J.A. van Mourik, J.
Dynamics and plasticity of Weibel-Palade bodies in endoth
Arterioscler. Thromb. Vasc. Biol. 26 (2006) 1002–1007.
[15] U. Fiedler, M. Scharpfenecker, S. Koidl, A. Hegen, V
J.M. Schmidt, W. Kriz, G. Thurston, H.G. Augustin, The T
angiopoietin-2 is stored in and rapidly released upon stimul
endothelial cell Weibel-Palade bodies, Blood 103 (2004) 415
[16] U. Fiedler, Y. Reiss, M. Scharpfenecker, V. Grunow,
G. Thurston, N.W. Gale, M. Witzenrath, S. Rosseau, N
A. Sobke, M. Herrmann, K.T. Preissner, P. Vajkoczy, H.G. Au
giopoietin-2 sensitizes endothelial cells to TNF-α and has a
in the induction of inflammation, Nat. Med. 12 (2006) 235–
[17] O. Dery, C.U. Corvera, M. Steinhoff, N.W. Bunnett, Proteinas
receptors: novel mechanisms of signaling by serine proteas
Physiol. 274 (1998) C1429–C1452.
[18] G. Cirino, C. Cicala, M.R. Bucci, L. Sorrentino, J.M. M
S.R. Stone, Thrombin functions as an inflammatory mediat
activation of its receptor, J. Exp. Med. 183 (1996) 821–827.
[19] G.P. van Nieuw Amerongen, S. van Delft, M.A. Vermeer, J.
V.W. van Hinsbergh, Activation of RhoA by thrombin in

hyperpermeability: role of Rho kinase and protein tyrosine kinases, Circ. Res. 87 (2000) 335–340.
[20] J.H. Cleator, W.Q. Zhu, D.E. Vaughan, H.E. Hamm, Differential regulation of endothelial exocytosis of P-selectin and von Willebrand factor by protease-activated receptors and cAMP, Blood 107 (2006) 2736–2744.
[21] S.C. Holt, L. Kesavalu, S. Walker, C.A. Genco, Virulence factors of *Porphyromonas gingivalis*, Periodontol. 2000 20 (1999) 168–238.
[22] B.W. Bainbridge, S.R. Coats, R.P. Darveau, *Porphyromonas gingivalis* lipopolysaccharide displays functionally diverse interactions with the innate host defense system, Ann. Periodontol. 7 (2002) 29–37.
[23] B.W. Bainbridge, R.P. Darveau, *Porphyromonas gingivalis* lipopolysaccharide: an unusual pattern recognition receptor ligand for the innate host defense system, Acta Odontol. Scand. 59 (2001) 131–138.
[24] G. Hajishengallis, A. Sharma, M.W. Russell, R.J. Genco, Interactions of oral pathogens with toll-like receptors: possible role in atherosclerosis, Ann. Periodontol. 7 (2002) 72–78.
[25] E. Burns, G. Bachrach, L. Shapira, G. Nussbaum, TLR2 is required for the innate response to *Porphyromonas gingivalis*: activation leads to bacterial persistence and TLR2 deficiency attenuates induced alveolar bone resorption, J. Immunol. 177 (2006) 8296–8300.
[26] A. Uehara, A. Iwashiro, T. Sato, S. Yokota, H. Takada, Antibodies to proteinase 3 prime human monocytic cells via protease-activated receptor-2 and NF-κB for toll-like receptor- and NOD-dependent activation, Mol. Immunol. 44 (2007) 3552–3562.
[27] S. Sugawara, A. Uehara, T. Nochi, T. Yamaguchi, H. Ueda, A. Sugiyama, K. Hanzawa, K. Kumagai, H. Okamura, H. Takada, Neutrophil proteinase 3-mediated induction of bioactive IL-18 secretion by human oral epithelial cells, J. Immunol. 167 (2001) 6568–6575.
[28] H.P. Hammes, J. Lin, P. Wagner, Y. Feng, F. vom Hagen, T. Krzizok, O. Renner, G. Breier, M. Brownlee, U. Deutsch, Angiopoietin-2 causes pericyte dropout in the normal retina: evidence for involvement in diabetic retinopathy, Diabetes 53 (2004) 1104–1110.

INFECTION AND IMMUNITY, May 2007, p. 2253–2259
0019-9567/07/$08.00+0 doi:10.1128/IAI.00141-07

Vol. 75, No. 5

Synthesis and Characterization of a Dipalmitoylated Lipopeptide Derived from Paralogous Lipoproteins of *Mycoplasma pneumoniae*▽†

Takeshi Into,[1]‡* Jun-ichi Dohkan,[1]‡ Megumi Inomata,[1] Misako Nakashima,[1] Ken-ichiro Shibata,[2] and Kenji Matsushita[1]

Department of Oral Disease Research, National Institute for Longevity Sciences, National Center for Geriatrics and Gerontology, Obu, Aichi, Japan,[1] and Laboratory of Oral Molecular Microbiology, Department of Oral Pathobiological Science, Hokkaido University Graduate School of Dental Medicine, Sapporo, Japan[2]

Received 28 January 2007/Accepted 12 February 2007

Genomic analysis of *Mycoplasma pneumoniae* revealed the existence of a large number of putative lipoprotein genes compared with the numbers in other bacteria. However, the pathogenic roles of *M. pneumoniae* lipoproteins are still obscure. In this study, we synthesized a lipopeptide (designated *M. pneumoniae* paralogous lipoprotein 1 [MPPL-1]) in which an *S*-dipalmitoylglyceryl cysteine was coupled to a peptide with a consensus sequence of a putative paralogous lipoprotein group characteristic of *M. pneumoniae*. The cytokine-inducing activity of MPPL-1 in human monocytic cells was much weaker (~700-fold weaker) than that of the known mycoplasmal *S*-dipalmitoylated lipopeptide FSL-1 or MALP-2. MPPL-1 required Toll-like receptor (TLR2) to activate NF-κB-dependent gene transcription in HEK293 cells, although a 1,000-fold-larger amount of MPPL-1 was needed to exert activity similar to that of FSL-1 in the cells. TLR2-mediated recognition of MPPL-1 was synergistically upregulated by TLR6 but not by TLR1 or TLR10, although the activity was still weak. In addition, MPPL-1 did not antagonize FSL-1 recognition in human monocytic cells and TLR2/TLR6-expressing HEK293 cells. Thus, these results suggest that there is preferential selective recognition of diacylated lipopeptides due to the magnitude of an affinity with TLR2 and TLR6 and the roles of increased paralogous lipoprotein genes of *M. pneumoniae* in evasion of TLR2 recognition.

Membrane-bound lipoproteins are thought to play important roles in the survival of bacteria through four main functions: a structural function, a transport function, an adhesion function, and an enzymatic function (7). Many lipoproteins have been identified in various species of bacteria and have been shown to comprise a framework structure containing a lipidated N-terminal cysteine residue coupled to distinct polypeptides. The maturation of bacterial lipoproteins generally comprises three steps; the first step involves diacylglyceryl modification of a cysteine residue by diacylglycerol transferase, the second step involves cleavage of the leader peptide by signal peptidase II, and the final step involves N acylation of the N-terminal diacylglyceryl cysteinyl residue, with which lipoproteins are synthesized as triacylated lipoproteins (7). It has also been shown that lipoproteins derived from *Rhodopseudomonas viridis* and several mycoplasmal species do not undergo modification in the final step and are synthesized as diacylated lipoproteins (7).

In contrast to their crucial functions in the survival of bacteria, bacterial lipoproteins act as pathogenic substances to stimulate the immune systems of humans and animals through the recognition receptors that monitor exogenous pathogens (3). Toll-like receptors (TLRs) are central pattern recognition receptors of the innate immune system that recognize a wide range of invading microorganisms through conserved chemical structures in their cells (34). TLR2 is essential for mediation of immune responses to the most diverse set of molecular structures of microbes, including peptidoglycans, lipoteichoic acids, porins, lipoarabinomannans, and lipoproteins/lipopeptides (21, 34). TLR2 forms heteromers with either TLR1 or TLR6, probably to discriminate the structures of molecular patterns, especially the N-terminal lipidated cysteinyl portions of bacterial lipoproteins as active sites (4, 29). TLR1 and TLR6 have been reported to be involved in simple discrimination of the difference between triacylated and diacylated lipoproteins/lipopeptides (36, 37). However, recent arduous work by several study groups has shown that such diverse potentials of TLR1 and TLR6 are largely dependent on more subtle structures of lipoproteins/lipopeptides, such as the length of an N-terminal fatty acid chain, the chirality of the central carbon of the diacylglycerol, and the charge of the C-terminal amino acids (5, 6, 28). It has been suggested that in addition to TLR1 and TLR6, TLR10, which is not encoded in the murine genome, is related to TLR2 recognition because of its sequence similarity and the possibility that it forms a heteromer with TLR2 (8, 12).

Mycoplasmas are microbes in regressive evolution and differ from other microbes in many respects. For example, they completely lack a cell wall, and their bilipid membrane is therefore the only structure that regulates interactions with the external environment (31). Some mycoplasmas cause severe respira-

* Corresponding author. Mailing address: Department of Oral Disease Research, National Institute for Longevity Sciences, National Center for Geriatrics and Gerontology, 36-3 Gengo, Morioka, Obu, Aichi 474-8522, Japan. Phone: 81-562-44-5651, ext. 5064. Fax: 81-562-46-8684. E-mail: into@nils.go.jp.

† Supplemental material for this article may be found at http://iai.asm.org/.

‡ T.I. and J.D. contributed equally to this work.

▽ Published ahead of print on 26 February 2007.

tory, arthritic, and urogenital diseases in humans and animals. *Mycoplasma pneumoniae* is a human pathogen that causes "atypical pneumonia," particularly in older children and young adults (38). The genome size of *M. pneumoniae* is ~820 kb, and the genomic sequence has been completely analyzed (13, 14). Interestingly, a large number of putative lipoprotein-encoding genes have been identified in the genome (46 of 689 genes; 6.68%) compared with the numbers of such genes in the genomes of other microbes, such as *Escherichia coli* K-12 (22 of 4,243 genes; 0.52%) and *Bacillus subtilis* (26 of 4,105 genes; 0.63%) (7). Even in the closely related sister species *Mycoplasma genitalium*, only 21 putative lipoproteins (encoded by 477 genes; 4.4%) could be found. Despite the existence of such genetic data, little is known about the roles of lipoproteins in *M. pneumoniae* pathogenicity, although there has been much interest in the pathogenic roles of membrane lipoproteins of other mycoplasmal species during infection because of their diverse functions, including adherence to host cells, antigenic variation, and TLR2- and TLR6-mediated immunostimulation (30).

In this study, we attempted to synthesize a lipopeptide having an *S*-(2,3-bispalmitoyloxypropyl)-cysteine residue coupled to an N-terminal consensus peptide of *M. pneumoniae*-specific lipoproteins encoded by paralogous genes. Interestingly, the level of immunostimulatory activity of this lipopeptide was much lower than that of the known mycoplasmal lipopeptide MALP-2 or FSL-1 despite the structural uniformity. We also investigated the recognition of this lipopeptide by TLRs.

MATERIALS AND METHODS

Preparation of synthetic lipopeptides. The synthetic lipopeptides FSL-1 and MALP-2 were prepared as described previously (17). *S*-(2,3-bisacyloxypropyl)-cysteinyl TGIQADLRNLIK, designated *M. pneumoniae* paralogous lipoprotein 1 (MPPL-1), was synthesized using a method similar to the method used for synthesis of FSL-1 and MALP-2. Briefly, the side chain-protected sequence TGIQADLRNLIK was constructed with an automated peptide synthesizer (model 433; Applied Biosystems). (9-Fluorenylmethoxy carbonyl)-*S*-(2,3-bispalmitoyloxypropyl)-cysteine (Novabiochem) was manually coupled to the peptide resin by using a 1-hydroxy-7-azabenzotriazole-1-ethyl-3-(3-dimethylaminopropyl)-carbodiimide/CH_2Cl_2-dimethylformamide solvent system. The 9-fluorenylmethoxy carbonyl and resin were removed from the lipopeptide by using trifluoroacetic acid. The lipopeptide was extracted into 90% acetic acid, lyophilized, and purified by preparative high-pressure liquid chromatography with a reversed-phase C_{18} column (30 by 250 mm). The level of purity of the lipopeptide was confirmed by analytical high-pressure liquid chromatography with a reversed-phase C_{18} column (4.6 by 150 mm) to be 96%. All of the lipopeptides were used without separation of the *S*-form and *R*-form stereoisomers. The lipopeptides were dissolved in phosphate-buffered saline containing 10 mM *n*-octyl-β-glucopyranoside at a concentration 0.5 mM and stored at −80°C until they were used.

Cell culture. Dulbecco modified Eagle medium, RPMI 1640 medium, penicillin G, streptomycin, and trypsin-EDTA were obtained from Sigma. Human monocytic cell line THP-1 was cultured in RPMI 1640 medium as described previously (19). Human embryonic kidney HEK293 cells were grown in Dulbecco modified Eagle medium as described previously (18).

Determination of IL-6 and IL-8 by enzyme-linked immunosorbent assays (ELISA). A total of 1×10^5 THP-1 cells were stimulated for 12 h with various concentrations of mycoplasmal lipopeptides, and the amounts of interleukin-6 (IL-6) and IL-8 released into the media were determined by using human IL-6 Cytoset and human IL-8 Cytoset (Invitrogen), respectively, according to the instructions of the manufacturer. The results described below are representative of three separate experiments, and the data are expressed as means and standard deviations.

DNA cloning. Plasmids encoding human TLR1, TLR2, and TLR6 have been described previously (18). Human TLR10 cDNA was obtained by reverse transcription-PCR of RNA isolated from human umbilical vein endothelial cells and then cloned into a pEF6 vector (Invitrogen). The DNA sequences were confirmed by the dideoxy chain termination method by using an ABI Prism 3 genetic analyzer.

Luciferase reporter gene assay. HEK293 cells were plated at a concentration of 0.5×10^5 cells per well in 24-well plates before transfection. The cells were transiently transfected with an NF-κB-driven firefly luciferase reporter plasmid (pNF-κB-Luc; Stratagene) and a construct directing expression of *Renilla* luciferase under the control of a constitutively active thymidine kinase promoter (pRL-TK; Promega) together with TLR-encoding plasmids. After 24 h of incubation, the cells were stimulated for 6 h with MPPL-1 or FSL-1 in medium containing 1% fetal bovine serum. Then the cells were lysed, and the luciferase activity was measured using the Dual-Luciferase reporter assay system (Promega) according to instructions of the manufacturer. The results below, expressed as the means and standard deviations of values for triplicate wells, are representative of three separate experiments. The experiment using HEK293 cells stably expressing TLR2 has been described previously (20).

Statistics. All values were evaluated by statistical analysis using Student-Newman-Keul's test. Differences were considered to be statistically significant at a P value of <0.05.

RESULTS

Preparation of MPPL-1. Himmelreich et al. reported that protein genes were identified as genes encoding putative lipoproteins in the *M. pneumoniae* M129 (=ATCC 29342) genome based on the following characteristic lipoprotein-specific features: (i) the presence of one or more basic amino acids among the first five to seven amino acids of the N terminus, (ii) the presence of a hydrophobic signal peptide, and (iii) the presence of a cysteine residue immediately downstream of the signal peptide (13). However, we found that 48 proteins lack these lipoprotein signatures. The N-terminal lipoprotein moieties of all putative lipoproteins are shown in Table S1 in the supplemental material. The amino acid sequences of these lipoproteins are included in the data at a website (http://www.ncbi.nlm.nih.gov/entrez/query.fcgi?CMD=search&DB=genome), and the protein designations were based on the MPN number scheme described by Himmelreich et al. (13). Importantly, many of these putative lipoproteins have recently been confirmed to be functionally expressed in the microorganism (11, 33, 39). In addition to 48 putative lipoproteins, there are several proteins with high levels of similarity to the lipoproteins without the lipoprotein signature at the N terminus (13), but we did not include these proteins in the list.

Comparison of 30 amino acids of N-terminal lipoprotein moieties revealed that the *M. pneumoniae* lipoproteins include members of seven subgroups, which are probably groups of paralogous lipoproteins (see Table S1 in the supplemental material). We focused on group 1 composed of MPN051, MPN054, MPN271, MPN369, MPN411, MPN467, MPN650, and MPN654 because the N-terminal sequences of these putative lipoproteins could not be identified by a BLAST search in other known organisms, even the sister species *M. genitalium*, suggesting that the lipoprotein genes were propagated uniquely in the evolution of this microorganism. The sequence of MPN505 is also very similar to the sequences of the lipoproteins, but MPN505 lacks the lipoprotein signature. Importantly, the study of Hallamaa et al. showed that there was expression of mRNAs for all group 1 lipoproteins and detectable proteins MPN271, MPN411, and MPN650 (20). Comparison of N-terminal sequences of these lipoproteins revealed that the levels of similarity of MPN271, MPN

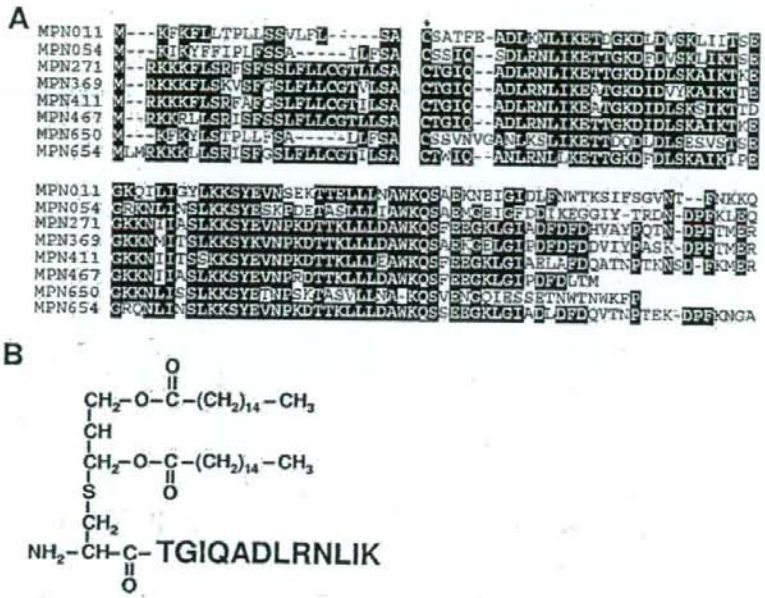

FIG. 1. Synthesis of MPPL-1. (A) Alignment of putative paralogous lipoproteins. The N-terminal sequences of MPN011, MPN054, MPN271, MPN369, MPN411, MPN467, MPN650, and MPN654 were compared. The cysteine residue immediately downstream of the signal peptide is indicated by an asterisk. (B) Structure of MPPL-1.

MPN411, MPN467, and MPN654 are particularly high (Fig. 1A). These putative lipoproteins have a characteristic feature; namely, the C-terminal amino acid residue flanking the cysteine residue immediately downstream of the signal peptide is threonine, although the corresponding amino acid of common bacterial lipoproteins is glycine, alanine, or serine.

To analyze the pathological roles of this paralogous lipoprotein group, we attempted to synthesize a lipopeptide having an N-terminal sequence common to these lipoproteins. The results of previous work suggested that synthetic lipopeptides with original peptide sequences with more than 10 amino acids could mimic the immunostimulatory activity of natural lipoproteins (24, 27, 32). Therefore, we determined that the partial consensus sequence of MPN271, MPN369, MPN411, MPN467, and MPN654 is TGIQADLRNLIK, which should couple to an *S*-dipalmitoylglyceryl cysteine. The structure was chemically synthesized using a method similar to the method used for synthesis of known mycoplasmal lipopeptides described previously (17, 32), and the protein was designated MPPL-1 (Fig. 1B). All of our preparations of mycoplasmal lipopeptides were synthesized as mixtures of the *S*-form and *R*-form stereoisomers.

Immunostimulatory activity of MPPL-1. To investigate the immunostimulatory activity of MPPL-1, we examined the induction of cytokine production in human monocytic THP-1 cells, comparing the activity of MPPL-1 with the activities of two synthetic mycoplasmal lipopeptides. MALP-2 (*S*-dipalmitoylglyceryl CGNNDESNISFKEK) derived from *Mycoplasma fermentans* was first identified and characterized by Mühlradt's group as a compound that can activate macrophages even at picomolar concentrations (24). FSL-1 (*S*-dipalmitoylglyceryl CGDPKHPKSF) derived from *Mycoplasma salivarium* has recently been characterized by our group as a potent immunostimulatory compound, whose activity has been proposed to be stronger than that of MALP-2 (16, 17, 27). MPPL-1 could induce production of IL-8 in a dose-dependent manner at a concentration of ≥10 nM, whereas FSL-1 and MALP-2 could induce the production of IL-8 at picomolar concentrations (Fig. 2A). To induce a level of IL-8 production similar to the level induced by 1 nM FSL-1, a 300-fold-higher concentration of MPPL-1 was required (Fig. 2A). Moreover, similar weak activity of MPPL-1 was also observed when IL-6 production in THP-1 cells was examined (Fig. 2B). In this case, the concentration of FSL-1 needed to induce a level of IL-6 production similar to that induced by 1 μM MPPL-1 was 700-fold lower (Fig. 2B). Thus, the immunostimulatory activity of MPPL-1 is much weaker than the activities of structurally similar lipopeptides.

TLR recognition of MPPL-1. It has been shown that FSL-1 and MALP-2 stimulate human cells via recognition by TLR2 and TLR6 (26, 27, 35). We first examined whether MPPL-1 was recognized by TLR2 using HEK293 cells intrinsically lacking expression of TLR2 and responsiveness to TLR2 ligands (1). MPPL-1 could not stimulate parental HEK293 cells at concentrations ranging from 100 fM to ~10 μM (data not shown) but could stimulate the cells stably transfected with TLR2, leading to induction of NF-κB activation, in a dose-dependent manner (Fig. 3A). Therefore, MPPL-1 recognition was completely dependent on TLR2 in the same way that FSL-1 and MALP-2 recognition was. However, an approximately 1,000-fold-higher concentration of MPPL-1 was re-

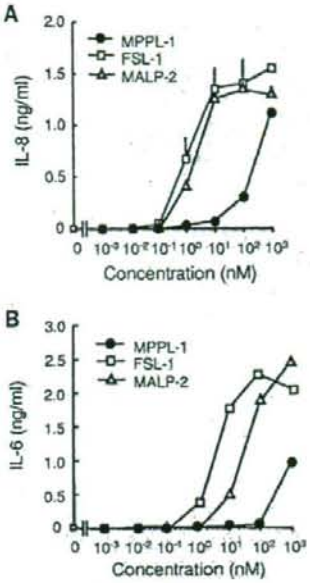

FIG. 2. Cytokine-inducing activity of MPPL-1. A total of 1×10^5 THP-1 cells were stimulated for 12 h with the concentrations of MPPL-1, FSL-1, and MALP-2 indicated. Then the amounts of IL-8 (A) and IL-6 (B) released into the media were determined by ELISA. The results are representative of three separate experiments, and the data are means and standard deviations.

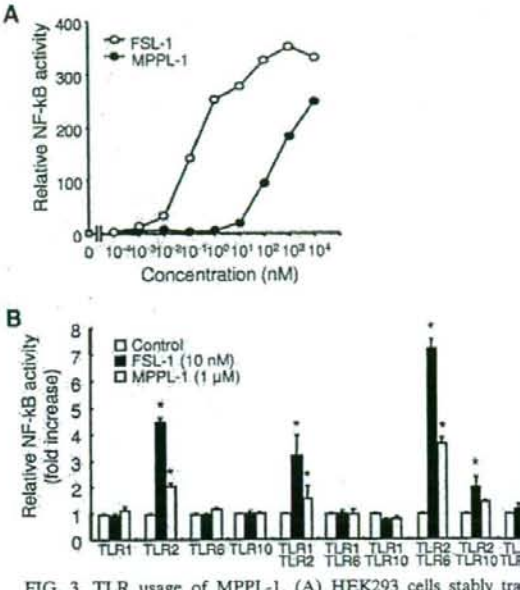

FIG. 3. TLR usage of MPPL-1. (A) HEK293 cells stably tra fected with TLR2 were prepared and transiently transfected with NF-κB-driven firefly luciferase reporter plasmid. The cells were st ulated for 6 h with the concentrations of MPPL-1 and FSL-1 indicat Then the cells were lysed, and the luciferase activity was measur The results, expressed as the means of values for triplicate wells, representative of three separate experiments. (B) HEK293 cells w transiently transfected with an NF-κB-driven firefly luciferase repo plasmid together with the TLR-encoding plasmids indicated. The c were stimulated for 6 h with 1 μM MPPL-1 or 10 nM FSL-1. Then cells were lysed, and the luciferase activity was measured. The resu expressed as means and standard deviations of values for triplic wells, are representative of three separate experiments. An aste indicates that the P value was <0.05 for a comparison with the con group.

quired for activity similar to that of FSL-1 in TLR2-expressing HEK293 cells (Fig. 3A).

We further investigated the requirement for TLR1, TLR6, and TLR10 for recognition of MPPL-1, since TLR2 has been shown to form not only a homomer but also heteromers with these TLRs (29). MPPL-1 could not activate HEK293 cells transfected with TLR1, TLR6, or TLR10 alone (Fig. 3B). Similarly, MPPL-1 could not activate cells transfected with a combination of TLR1 and TLR6, TLR1 and TLR10, or TLR6 and TLR10 (Fig. 3B). Compared with the MPPL-1 activity in the cells transfected with TLR2 alone, cotransfection of TLR6 with TLR2 synergically augmented the activity of MPPL-1 in a way similar to way observed with FSL-1, whereas cotransfection of TLR1 or TLR10 with TLR2 did not (Fig. 3B). Thus, MPPL-1 is preferentially recognized by TLR2/TLR6 in human cells in a manner similar to the recognition of FSL-1 and MALP-2.

Possibility of an antagonistic effect of MPPL-1 on TLR2 recognition. TLR4 recognition of *E. coli* lipopolysaccharide can be antagonized by structurally similar compounds that have weak TLR4-stimulating activities (9, 10, 23, 25). However, it is still not clear whether TLR2 recognition of lipopeptides can be antagonized by structurally similar compounds. The results described above raise the possibility that MPPL-1 has an antagonistic effect on FSL-1 recognition by TLR2/TLR6, because MPPL-1 exhibits a much lower level of activity than FSL-1 exhibits through recognition by TLR2/TLR6. We therefore examined the IL-6-producing activity of FSL-1 in the presence and absence of a higher concentration of MPPL-1. IL-6 production induced by 1 or 10 nM FSL-1 was not alte by the presence of 1 μM MPPL-1 (Fig. 4A). Moreover, presence of MPPL-1 was found to slightly increase the acti of FSL-1 as determined by analysis of NF-κB activation HEK293 cells (Fig. 4B), and this analysis was more sensit than an IL-6 ELISA with THP-1 cells. In addition, the MPP effect on FSL-1 recognition was not altered in the presence absence of TLR1, TLR6, or TLR10 cotransfection (Fig. 4 Similar results were obtained in experiments using MAL (data not shown).

DISCUSSION

We have been interested in the immunostimulatory acti of mycoplasmal diacylated lipoproteins/lipopeptides and pathological roles of these proteins in mycoplasmal infectio So far, lipopeptides FSL-1 and MALP-2 have been identif as potent immunostimulatory compounds (22, 24). In t study, we synthesized lipopeptide MPPL-1 having a struct common in mycoplasmal lipopeptides, an *S*-dipalmitoylglyce cysteine residue coupled to a distinct peptide, which determined on the basis of paralogous lipoproteins char

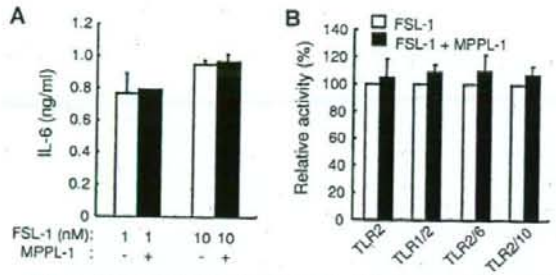

FIG. 4. Antagonistic effect of MPPL-1. (A) A total of 1×10^5 THP-1 cells were stimulated for 12 h with 1 or 10 nM FSL-1 in the presence or absence of 1 μM MPPL-1. Then the amounts of IL-6 released into the media were determined by ELISA. The results, expressed as means and standard deviations, are representative of three separate experiments. (B) HEK293 cells were transiently transfected with an NF-κB-driven firefly luciferase reporter plasmid together with the TLR-encoding plasmids indicated. The cells were stimulated for 6 h with 1 nM FSL-1 in the presence or absence of 100 nM MPPL-1. Then the cells were lysed, and the luciferase activity was measured. The results, expressed as means and standard deviations of values for triplicate wells, are representative of three separate experiments.

teristic of *M. pneumoniae*. The cytokine-inducing activity of MPPL-1 in human cells was very weak compared with that of FSL-1 or MALP-2. At a higher concentration, MPPL-1 could weakly stimulate cells via TLR2/TLR6 recognition. However, MPPL-1 could not antagonize FSL-1 recognition by TLR2. These findings raised several important possibilities for biological activities of mycopalsmal lipopeptides, as discussed below.

Recent studies have revealed that the immunostimulatory activity of bacterial lipoproteins is completely dependent on the recognition and signal transduction by TLR2 that functions together with several associated molecules. TLR6 has been considered to be an essential participant in the discrimination of mycoplasmal diacylated lipoproteins/lipopeptides by TLR2, because MALP-2 recognition was impaired in macrophages from TLR6-deficient mice (36) and was reduced by a blocking antibody to TLR6 in human cells (26). However, Buwitt-Beckmann et al. found that C-terminal addition of SKKKK to the peptide moiety of MALP-2 converted the MALP-2 recognition by TLR2/TLR6 into recognition by a TLR6-independent mechanism (6). In addition, we previously reported that substitution of the C-terminal amino acid of FSL-1 (F to R) greatly impaired the immunostimulatory activity (27). Therefore, discrimination of diacylated lipopeptides by TLR2 and TLR6 has been suggested to be dependent on the amino acid sequence or structure of the peptide portion, although recognition of the lipolyated cysteine residue may be dependent on other molecules, such as CD36 (15). Furthermore, a recent report suggested that TLR1 participates in the recognition of a dipalmitoylated lipoprotein derived from *M. pneumoniae* (MPN602) (33). In this study, MPPL-1 was shown to be recognized by TLR2 and TLR6 but not by TLR1 or TLR10, as observed for MALP-2 and FSL-1. We could not discern a role for TLR10 in the recognition of mycoplasmal lipopeptides, although it is possible that TLR10 participates in accurate discrimination of bacterial lipoproteins/lipopeptides in human cells.

It is possible that studies of TLR antagonists may lead to the development of efficient therapeutic regulators of microbial infection or excess inflammation. In this study, however, MPPL-1 could not antagonize TLR2 recognition of FSL-1 (Fig. 4). The weak TLR2-stimulating activity of MPPL-1 raises the possibility that the peptide moiety of MPPL-1 has a low affinity for TLR6 but does not have an affinity for either TLR1 or TLR10. This possibility may be supported by our results showing that a small amount of FSL-1, which may have a stronger affinity than MPPL-1 has, could be preferentially recognized by TLR2 and TLR6 more than a larger amount of MPPL-1 could be recognized (Fig. 4). Moreover, our results may provide strong evidence for different ligand recognition mechanisms of TLR2 and TLR4, because TLR4 recognition of lipopolysaccharide is known to be antagonized by structurally similar compounds that have weak TLR4-stimulating activities (9, 10, 23, 25). Further study is needed to determine the detailed recognition machinery of mycoplasmal lipoproteins/lipopeptides.

The magnitude of the immunostimulatory activity of bacterial lipoproteins has been thought to be one of the crucial factors for pathogenicity of bacteria (3) which may be involved in the severity of host immune responses after bacterial infection. However, the presence of immunostimulatory compounds on the surface of bacterial cells leads to efficient clearance of bacteria through activation of immune cells, resulting in great reductions in efficient propagation and colonization on the host cell surface. To avoid activation of immune responses, several pathogenic bacteria have been shown to modify their surface molecules so they do not stimulate the TLR recognition system. For example, α- and ε-*Proteobacteria*, including *Campylobacter jejuni*, *Helicobacter pylori*, and *Bartonella bacilliformis*, modify the N-terminal D1 domain of flagellin, leading to evasion of TLR5 recognition (2). Therefore, structural modification of pathogen-activated molecular patterns may be important for bacterial pathogenicity. However, it has not been determined whether *M. pneumoniae* has the ability to evade immune systems. So far, mycoplasmal lipoproteins/lipopeptides have been identified to determine strong activators of immune cells in crude mixtures of lipoproteins obtained using methods such as Triton X-114 phase separation (24, 32, 33). In a recent study performed by Shimizu et al. (33), lipoprotein MPN602, which may have the strongest activities in *M. pneumoniae* lipoprotein mixtures, was identified by using a method to separate the fraction that strongly stimulates 293T cells transfected with TLR2 to activate NF-κB (33). MPN602 does not belong to a paralogous lipoprotein family, as shown in Table S1 in the supplemental material. Interestingly, it was also found that only a few lipoproteins possessed strong immunostimulatory activities and that the majority of lipoproteins had weak or no immunostimulatory activity (24, 32, 33). Consistent with this possibility, only a few lipoproteins with potent immunostimulatory activity have been identified so far, although there are many lipoproteins in mycoplasmal species. These observations suggest that the majority of lipoproteins of *M. pneumoniae*, including paralogous lipoprotein family members, have weak immunostimulatory activities. Moreover, our results suggest that propagation of genes encoding lipoproteins with

weak immunostimulatory activity may be an important factor for the pathogenicity of *M. pneumoniae* through which the microorganism may evade TLR2 recognition. Further detailed investigations of the functions and immunostimulatory activities of lipoproteins found in *M. pneumoniae* are needed to address this possibility.

The bacterial lipoprotein structure has been found to be a lipidated (commonly palmitoylated) triacylated or diacylated *S*-glyceryl cysteine residue coupled to distinct polypeptides. However, the coupled peptide sequence has been shown to have a great effect on the immunostimulatory activity of the whole molecule. Therefore, synthesis and characterization of lipopeptides based on the known lipoprotein sequences of the N terminus may be an effective method for determining unknown biological activities of bacterial lipoproteins. Moreover, exhaustive screening of synthetic lipopeptides can lead to the identification of novel bacterial pathogenicities and to the development of biologically beneficial compounds or immune regulators. Also, it is possible that a cognate ligand for TLR10 will be identified by screening of these lipopeptides.

ACKNOWLEDGMENTS

This work was supported by grants-in-aid for young scientists (B): 16791102 and (B):18791363 to T.I. provided by the Ministry of Education, Culture, Sports, Science and Technology, Japan.

REFERENCES

1. **Aliprantis, A. O., R. B. Yang, M. R. Mark, S. Suggett, B. Devaux, J. D. Radolf, G. R. Klimpel, P. Godowski, and A. Zychlinsky.** 1999. Cell activation and apoptosis by bacterial lipoproteins through Toll-like receptor-2. Science **285**:736–739.
2. **Andersen-Nissen, E., K. D. Smith, K. L. Strobe, S. L. Barrett, B. T. Cookson, S. M. Logan, and A. Aderem.** 2005. Evasion of Toll-like receptor 5 by flagellated bacteria. Proc. Natl. Acad. Sci. USA **102**:9247–9252.
3. **Brightbill, H. D., D. H. Libraty, S. R. Krutzik, R. B. Yang, J. T. Belisle, J. R. Bleharski, M. Maitland, M. V. Norgard, S. E. Plevy, S. T. Smale, P. J. Brennan, B. R. Bloom, P. J. Godowski, and R. L. Modlin.** 1999. Host defense mechanisms triggered by microbial lipoproteins through Toll-like receptors. Science **285**:732–736.
4. **Bulut, Y., E. Faure, L. Thomas, O. Equils, and M. Arditi.** 2001. Cooperation of Toll-like receptor 2 and 6 for cellular activation by soluble tuberculosis factor and *Borrelia burgdorferi* outer surface protein A lipoprotein: role of Toll-interacting protein and IL-1 receptor signaling molecules in Toll-like receptor 2 signaling. J. Immunol. **167**:987–994.
5. **Buwitt-Beckmann, U., H. Heine, K. H. Wiesmuller, G. Jung, R. Brock, S. Akira, and A. J. Ulmer.** 2006. TLR1- and TLR6-independent recognition of bacterial lipopeptides. J. Biol. Chem. **281**:9049–9057.
6. **Buwitt-Beckmann, U., H. Heine, K. H. Wiesmuller, G. Jung, R. Brock, S. Akira, and A. J. Ulmer.** 2005. Toll-like receptor 6-independent signaling by diacylated lipopeptides. Eur. J. Immunol. **35**:282–289.
7. **Chambaud, I., H. Wroblewski, and A. Blanchard.** 1999. Interactions between mycoplasma lipoproteins and the host immune system. Trends Microbiol. **7**:493–499.
8. **Chuang, T., and R. J. Ulevitch.** 2001. Identification of hTLR10: a novel human Toll-like receptor preferentially expressed in immune cells. Biochim. Biophys. Acta **1518**:157–161.
9. **Coats, S. R., T. T. Pham, B. W. Bainbridge, R. A. Reife, and R. P. Darveau.** 2005. MD-2 mediates the ability of tetra-acylated and penta-acylated lipopolysaccharides to antagonize *Escherichia coli* lipopolysaccharide at the TLR4 signaling complex. J. Immunol. **175**:4490–4498.
10. **Coats, S. R., R. A. Reife, B. W. Bainbridge, T. T. Pham, and R. P. Darveau.** 2003. *Porphyromonas gingivalis* lipopolysaccharide antagonizes *Escherichia coli* lipopolysaccharide at Toll-like receptor 4 in human endothelial cells. Infect. Immun. **71**:6799–6807.
11. **Hallamaa, K. M., G. F. Browning, and S. L. Tang.** 2006. Lipoprotein multigene families in *Mycoplasma pneumoniae*. J. Bacteriol. **188**:5393–5399.
12. **Hasan, U., C. Chaffois, C. Gaillard, V. Saulnier, E. Merck, S. Tancredi, C. Guiet, F. Briere, J. Vlach, S. Lebecque, G. Trinchieri, and E. E. Bates.** 2005. Human TLR10 is a functional receptor, expressed by B cells and plasmacytoid dendritic cells, which activates gene transcription through MyD88. J. Immunol. **174**:2942–2950.
13. **Himmelreich, R., H. Hilbert, H. Plagens, E. Pirkl, B. C. Li, and Herrmann.** 1996. Complete sequence analysis of the genome of the b terium *Mycoplasma pneumoniae*. Nucleic Acids Res. **24**:4420–4449.
14. **Himmelreich, R., H. Plagens, H. Hilbert, B. Reiner, and R. Herrmann.** 19 Comparative analysis of the genomes of the bacteria *Mycoplasma pn moniae* and *Mycoplasma genitalium*. Nucleic Acids Res. **25**:701–712.
15. **Hoebe, K., P. Georgel, S. Rutschmann, X. Du, S. Mudd, K. Crozat, S. Sova L. Shamel, T. Hartung, U. Zahringer, and B. Beutler.** 2005. CD36 is a sen of diacylglycerides. Nature **433**:523–527.
16. **Hubschle, T., J. Mutze, P. F. Muhlradt, S. Korte, R. Gerstberger, and Roth.** 2006. Pyrexia, anorexia, adipsia, and depressed motor activity in during systemic inflammation induced by the Toll-like receptors-2 and agonists MALP-2 and FSL-1. Am. J. Physiol. Regul. Integr. Comp. Phys **290**:R180–187.
17. **Into, T., M. Fujita, T. Okusawa, A. Hasebe, M. Morita, and K. Shibata.** 2 Synergic effects of mycoplasmal lipopeptides and extracellular ATP on tivation of macrophages. Infect. Immun. **70**:3586–3591.
18. **Into, T., K. Kiura, M. Yasuda, H. Kataoka, N. Inoue, A. Hasebe, K. Takeda Akira, and K. Shibata.** 2004. Stimulation of human Toll-like receptor (TL and TLR6 with membrane lipoproteins of *Mycoplasma fermentans* induce optotic cell death after NF-κB activation. Cell. Microbiol. **6**:187–199.
19. **Into, T., Y. Nodasaka, A. Hasebe, T. Okuzawa, J. Nakamura, N. Ohata, K. Shibata.** 2002. Mycoplasmal lipoproteins induce Toll-like receptor 2- caspases-mediated cell death in lymphocytes and monocytes. Microbiol. munol. **46**:265–276.
20. **Into, T., and K. Shibata.** 2005. Apoptosis signal-regulating kinase 1-m ated sustained p38 mitogen-activated protein kinase activation regul mycoplasmal lipoprotein- and staphylococcal peptidoglycan-triggered T like receptor 2 signalling pathways. Cell. Microbiol. **7**:1305–1317.
21. **Kirschning, C. J., and R. R. Schumann.** 2002. TLR2: cellular sensor microbial and endogenous molecular patterns. Curr. Top. Microbiol. Im nol. **270**:121–144.
22. **Kiura, K., H. Kataoka, T. Nakata, T. Into, M. Yasuda, S. Akira, N. In and K. Shibata.** 2006. The synthetic analogue of mycoplasmal lipopro FSL-1 induces dendritic cell maturation through Toll-like receptor 2. FE Immunol. Med. Microbiol. **46**:78–84.
23. **Lepper, P. M., M. Triantafilou, C. Schumann, E. M. Schneider, and Triantafilou.** 2005. Lipopolysaccharides from *Helicobacter pylori* can ac antagonists for Toll-like receptor 4. Cell. Microbiol. **7**:519–528.
24. **Mühlradt, P. F., M. Kiess, H. Meyer, R. Sussmuth, and G. Jung.** 1 Isolation, structure elucidation, and synthesis of a macrophage stimula lipopeptide from *Mycoplasma fermentans* acting at picomolar concentrat J. Exp. Med. **185**:1951–1958.
25. **Mullarkey, M., J. R. Rose, J. Bristol, T. Kawata, A. Kimura, S. Kobaya M. Przetak, J. Chow, F. Gusovsky, W. J. Christ, and D. P. Rossignol.** 2 Inhibition of endotoxin response by e5564, a novel Toll-like receptor rected endotoxin antagonist. J. Pharmacol. Exp. Ther. **304**:1093–1102.
26. **Nakao, Y., K. Funami, S. Kikkawa, M. Taniguchi, M. Nishiguchi, Y. Fukui T. Seya, and M. Matsumoto.** 2005. Surface-expressed TLR6 participates i recognition of diacylated lipopeptide and peptidoglycan in human cells. J. munol. **174**:1566–1573.
27. **Okusawa, T., M. Fujita, J. Nakamura, T. Into, M. Yasuda, A. Yoshimur Hara, A. Hasebe, D. T. Golenbock, M. Morita, Y. Kuroki, T. Ogawa, an Shibata.** 2004. Relationship between structures and biological activitie mycoplasmal diacylated lipopeptides and their recognition by Toll-like ceptors 2 and 6. Infect. Immun. **72**:1657–1665.
28. **Omueti, K. O., J. M. Beyer, C. M. Johnson, E. A. Lyle, and R. I. Tapp** 2005. Domain exchange between human Toll-like receptors 1 and 6 rev a region required for lipopeptide discrimination. J. Biol. Chem. **280**:36 36625.
29. **Ozinsky, A., D. M. Underhill, J. D. Fontenot, A. M. Hajjar, K. D. Sm C. B. Wilson, L. Schroeder, and A. Aderem.** 2000. The repertoire for pat recognition of pathogens by the innate immune system is defined by c eration between Toll-like receptors. Proc. Natl. Acad. Sci. USA **97**:13 13771.
30. **Rawadi, G.** 2000. *Mycoplasma fermentans* interaction with monocytes/ rophages: molecular basis. Microbes Infect. **2**:955–964.
31. **Rottem, S.** 2003. Interaction of mycoplasmas with host cells. Physiol. **83**:417–432.
32. **Shibata, K., A. Hasebe, T. Into, M. Yamada, and T. Watanabe.** 2000. N-terminal lipopeptide of a 44-kDa membrane-bound lipoprotein of *M plasma salivarium* is responsible for the expression of intercellular adhe molecule-1 on the cell surface of normal human gingival fibroblasts. J. munol. **165**:6538–6544.
33. **Shimizu, T., Y. Kida, and K. Kuwano.** 2005. A dipalmitoylated lipopro from *Mycoplasma pneumoniae* activates NF-κB through TLR1, TLR2, TLR6. J. Immunol. **175**:4641–4646.
34. **Takeda, K., T. Kaisho, and S. Akira.** 2003. Toll-like receptors. Annu. Immunol. **21**:335–376.
35. **Takeuchi, O., A. Kaufmann, K. Grote, T. Kawai, K. Hoshino, M. Morr, Muhlradt, and S. Akira.** 2000. Preferentially the *R*-stereoisomer of mycoplasmal lipopeptide macrophage-activating lipopeptide-2 activates

mune cells through a Toll-like receptor 2- and MyD88-dependent signaling pathway. J. Immunol. 164:554–557.
36. **Takeuchi, O., T. Kawai, P. F. Muhlradt, M. Morr, J. D. Radolf, A. Zychlinsky, K. Takeda, and S. Akira.** 2001. Discrimination of bacterial lipoproteins by Toll-like receptor 6. Int. Immunol. 13:933–940.
37. **Takeuchi, O., S. Sato, T. Horiuchi, K. Hoshino, K. Takeda, Z. Dong, R. L. Modlin, and S. Akira.** 2002. Role of Toll-like receptor 1 in mediating immune response to microbial lipoproteins. J. Immunol. 169:10–14.
38. **Waites, K. B., and D. F. Talkington.** 2004. *Mycoplasma pneumoniae* and its role as a human pathogen. Clin. Microbiol. Rev. 17:697–728.
39. **Weiner, J., 3rd, R. Herrmann, and G. F. Browning.** 2000. Transcription in *Mycoplasma pneumoniae*. Nucleic Acids Res. 28:4488–4496.

Editor: D. L. Burns

THE JOURNAL OF BIOLOGICAL CHEMISTRY VOL. 282, NO. 11, pp. 8134–8141, March 16, 2007

Pathogen Recognition by Toll-like Receptor 2 Activates Weibel-Palade Body Exocytosis in Human Aortic Endothelial Cells*

Received for publication, October 24, 2006, and in revised form, December 22, 2006 Published, JBC Papers in Press, January 16, 2007, DOI 10.1074/jbc.M609962200

Takeshi Into[‡1], Yosuke Kanno[‡], Jun-ichi Dohkan[‡], Misako Nakashima[‡], Megumi Inomata[‡], Ken-ichiro Shibata[§], Charles J. Lowenstein[¶], and Kenji Matsushita[‡]

From the [‡]Department of Oral Disease Research, National Institute for Longevity Sciences, National Center for Geriatrics and Gerontology, 36-3 Gengo, Morioka, Obu, Aichi 474-8522, Japan, the [§]Laboratory of Oral Molecular Microbiology, Department of Oral Pathobiological Science, Hokkaido University Graduate School of Dental Medicine, Sapporo 060-8586, Japan, and the [¶]Departments of Medicine and Pathology, Johns Hopkins University School of Medicine, Baltimore, Maryland 21205

The endothelial cell-specific granule Weibel-Palade body releases vasoactive substances capable of modulating vascular inflammation. Although innate recognition of pathogens by Toll-like receptors (TLRs) is thought to play a crucial role in promotion of inflammatory responses, the molecular basis for early-phase responses of endothelial cells to bacterial pathogens has not fully been understood. We here report that human aortic endothelial cells respond to bacterial lipoteichoic acid (LTA) and synthetic bacterial lipopeptides, but not lipopolysaccharide or peptidoglycan, to induce Weibel-Palade body exocytosis, accompanied by release or externalization of the storage components von Willebrand factor and P-selectin. LTA could activate rapid Weibel-Palade body exocytosis through a TLR2- and MyD88-dependent mechanism without *de novo* protein synthesis. This process was at least mediated through MyD88-dependent phosphorylation and activation of phospholipase Cγ. Moreover, LTA activated interleukin-1 receptor-associated kinase-1-dependent delayed exocytosis with *de novo* protein synthesis and phospholipase Cγ-dependent activation of the NF-κB pathway. Increased TLR2 expression by transfection or interferon-γ treatment increased TLR2-mediated Weibel-Palade body exocytosis, whereas reduced TLR2 expression under laminar flow decreased the response. Thus, we propose a novel role for TLR2 in induction of a primary proinflammatory event in aortic endothelial cells through Weibel-Palade body exocytosis, which may be an important step for linking innate recognition of bacterial pathogens to vascular inflammation.

The onset of inflammatory responses of vascular endothelial cells plays crucial roles in recruitment of immune cells, thrombus formation, and development of vascular inflammation or atherosclerosis. Early endothelial activation involves dual phases: rapid translocation of P-selectin to the endothelial surface and slower synthesis and expression of adhesion molecules such as ICAM-1 (intercellular adhesion molecule 1).[2] The former process is accompanied by rapid exocytosis of Weibel-Palade bodies, which are endothelial cell-specific storage granules that contain vascular modulators, including von Willebrand factor (VWF), P-selectin, IL-8, eotaxin-3, endothelin-1, CD63/lamp3, osteoprotegerin, and angiopoietin-2 (1, 2). During Weibel-Palade body exocytosis, these proteins are transported to the outside of the cell upon stimulation or vascular damage and may control local or systemic pathobiological effects, including thrombosis and atherogenesis. Regulated Weibel-Palade body exocytosis is known to be initiated through an increase of intracellular calcium level after stimulation with various secretagogues, including calcium ionophores, thrombin, histamine, TNF-α, and extracellular ATP (1, 2).

Recently, excess innate immune responses of vessel walls or endothelium to invading pathogens have been suggested to be linked to atherogenesis. Several common bacterial infectious agents or invasive pathogens, such as *Chlamydia pneumoniae*, *Helicobacter pylori*, *Porphyromonas gingivalis*, and oral commensal bacteria, have so far been detected in vessel walls or atherosclerotic lesions in humans (3, 4). However, the linkage between artery endothelial innate recognition of such pathogens and inflammatory responses has not been fully elucidated.

For the detection of invasive bacteria in host defense, several Toll-like receptors (TLRs) are employed to identify molecular motifs that usually compose bacterial bodies (5). Among TLR members in humans, TLR2 detects the widest range of common bacterial constituents, such as lipoteichoic acids (LTA),

* This work was supported by a Grant-in-aid for Young Scientists ((B):18791363 to T. I.) provided by the Ministry of Education, Culture, Sports, Science and Technology and by Mitsui, Life Social Welfare Foundation, Aich Cancer Research Foundation, Mitsubishi Pharma Research Foundation, Mochida Memorial Foundation for Medical and Pharmaceutical Research, and Suzuken Memorial Foundation (to K. M.). The costs of publication of this article were defrayed in part by the payment of page charges. This article must therefore be hereby marked "*advertisement*" in accordance with 18 U.S.C. Section 1734 solely to indicate this fact.

[1] To whom correspondence should be addressed. Tel.: 81-562-44-5651; Fax: 81-562-46-8684; E-mail: into@nils.go.jp.

[2] The abbreviations used are: ICAM-1, intercellular adhesion molecule 1; BAPTA-AM, 1,2-bis(2-aminophenoxy)ethane-*N,N,N′,N′*-tetraacetic acid-acetoxymethyl ester; FSL-1, synthetic *S*-dipalmitoylglyceryl-CGDPKHPKSF derived from *Mycoplasma salivarium*; HAEC, human aortic endothelial cell; HUVEC, human umbilical vein endothelial cell; IRAK, IL-1R-associated kinase; LTA, lipoteichoic acid; MALP-2, synthetic *S*-dipalmitoylglyceryl-CGNNDESNISFKEK derived from *Mycoplasma fermentans*; Pam_3CSK_4, synthetic *N*-palmitoyl-*S*-dipalmitoylglyceryl-CSKKKK derived from *E. coli*; PGN, peptidoglycan; PLC, phospholipase C; TLR, Toll-like receptor; TNF, tumor necrosis factor; TNFR, TNF receptor; TRAF, TNFR-associated factor; VWF, von Willebrand factor; LPS, lipopolysaccharide; IL-1R, interleukin-1 receptor; siRNA, small interference RNA; ELISA, enzyme-linked immunosorbent assay; PI3K, phosphatidylinositol 3-kinase; IFN, interferon.

peptidoglycans (PGN), bacterial di- or triacylated lipoproteins or lipopeptides, lipoarabinomannans, porins, and fimbriae (5–8). TLR4 and TLR5 contribute to the recognition of only a few bacterial components, *i.e.* LPS and flagellin (9, 10). Because TLR1 and TLR6 participate in the accurate discrimination of molecular structures by TLR2 as coreceptors, several molecules, including CD14, CD36, and LOX-1, further facilitate the interactions of TLR2 with bacterial pathogens (5, 11, 12). After recognition of cognate agonists, endothelial TLRs activate the classic Toll/IL-1R signaling pathway utilizing MyD88 and IL-1R-associated kinase (IRAK)-1, which ultimately activate a TNFR-associated factor (TRAF) 6 complex and IκBs and the release and translocation of active NF-κB to the nucleus. The artery endothelial NF-κB signaling pathways downstream of TLRs are thought to participate in the development of artery inflammatory diseases or atherogenesis through the promotion of the expression of a large number of proinflammatory mediators and adhesion molecules (13–15). However, it is still not known whether artery endothelial TLRs are primary initiators or modulators of the diseases.

In this study, we investigated the early-phase proinflammatory responses of human aortic endothelial cells (HAECs) to bacterial cell wall constituents. We found that recognition of bacterial constituents by TLRs, especially by TLR2 but not TLR4, could activate Weibel-Palade body exocytosis. We further investigated the involvement of MyD88 in regulation of the cell response.

EXPERIMENTAL PROCEDURES

Reagents, Chemicals, and Antibodies—LTA and PGN from *Staphylococcus aureus* and LPS from *Escherichia coli* O26:B6 were obtained from Sigma-Aldrich. Rough-form LPS from *Salmonella minnesota* R595 and flagellin from *Salmonella typhimurium* strain 14028 were obtained from Alexis Biochemicals. Pam_3CSK_4 (16) was obtained from InvivoGen. Preparation of FSL-1 and MALP-2 was described previously (17–19). A23187, the cell-permeable calcium chelator 1,2-bis(2-aminophenoxy)ethane-*N*,*N*,*N*′,*N*′-tetraacetic acid-acetoxymethyl ester (BAPTA-AM), cycloheximide, and the phospholipase C (PLC) γ inhibitor U-73122 were purchased from Sigma. LY294002 was purchased from Calbiochem. Monoclonal antibodies to human TLR2, TL2.1 (BD Biosciences), TL2.3 (eBioscience), and IMG-319 (Immugenex), were purchased for a TLR2 blocking study and flow cytometry. Antibodies to PLCγ1 and phosphorylated PLCγ1 (Y783) were obtained from Cell Signaling Biotechnology. All other reagents were obtained from Sigma-Aldrich unless otherwise indicated.

DNA Cloning—A human TLR2-encoding plasmid was prepared as described previously (17). The dominant negative TLR2 (P681H) was constructed using a QuikChange II site-directed mutagenesis kit (Stratagene) according to the manufacturer's instructions.

Cell Culture and Transfection of siRNA—HEK293 cells and human monocytic THP-1 cells were grown as described previously (20). HAECs and HUVECs were grown in endothelial growth medium-2 (Camblex) as described previously (21). These endothelial cells were used for experiments from passages 4 to 8. All of the gene-specific siRNA oligonucleotides for human TLR1, TLR2, TLR6, MyD88, and IRAK-1 and a c oligonucleotide were purchased from Dharmacon. Alt the sequences were not provided by the manufacturer, cant suppressive effects on the respective gene expressio be confirmed by reverse transcription-PCR compared w control transfection (data not shown). For the transfec siRNA, confluent HAECs or HUVECs seeded on 6- or plates were prepared and washed once with Opti-M medium (Invitrogen). Transfection of siRNAs (100 n performed with Lipofectin reagent (Invitrogen) as instru the manufacturer. Toxi-Blocker transfection supp (TOYOBO) was used to prevent cytotoxicity of lipo reagents. After 12 h of incubation, culture media were c to endothelial growth medium-2 media, and incubati continued for 24 h.

Luciferase Reporter Gene Assay—HEK293 cells stably fected with human TLR2 gene (or mock control vecto plated at 5×10^4 cells/well in 24-well plates before DNA fection. The cells were transiently transfected with 50 n NF-κB-driven firefly luciferase reporter plasmid (pNF-κ Stratagene) and 5 ng of a construct directing expres *Renilla* luciferase under the control of a constitutively thymidine kinase promoter (pRL-TK, Promega). After incubation, the cells were transfected with 100 nM siRN gonucleotide for MyD88 (or glyceraldehyde-3-pho dehydrogenase control). Toxi-Blocker transfection ment was used to prevent cytotoxicity of lipofection re After a further 24 h of incubation, the cells were stimulat TLR2 agonists in media containing 1% fetal bovine ser 6 h. Then the cells were lysed, and luciferase activity wa ured as described previously (17, 20).

Determination of VWF, IL-8, and TNF-α by ELISA—H were grown on 24-well plates, then washed and placed in of Opti-Mem I (Invitrogen) containing 1% fetal bovine without growth factors, and stimulated with various con tions of TLR2 agonists for 60 min. The amount of VWF r into the medium was measured by a VWF ELISA kit (Am Diagnostica) according to the manufacturer's instru Results are representative of three separate experimen expressed as means ± S.D. To clarify the mechanism by TLR2 induces VWF exocytosis, HAECs were pretreated min with 10 μM U-73211 and then stimulated with LTA min. For other experiments, HAECs were pretreated μM BAPTA-AM for 30 min or 10 ng/ml IFN-γ for precultured with $CaCl_2$-free DMEM for 1 h. To determ amounts of IL-8 released, HAECs were grown on 96-wel and then washed and placed in 200 μl of Opti-Mem I (I gen) containing 1% fetal bovine serum and stimulated with various concentrations of TLR2 agonists. The amo IL-8 released into the media were measured by huma Cytoset (Invitrogen) according to the manufacturer's i tions. THP-1 cells (1×10^5) were stimulated for 6 h with concentrations of TLR2 agonists. The amounts of released into the media were measured by human TNF-α set (Invitrogen) according to the manufacturer's instru Results are representative of three separate experimen expressed as means ± S.D.

Adhesion Assay—Confluent HAECs seeded on 24-well plates were treated with 10 μg/ml LTA for 60 min. The culture medium was then removed, and monocytic THP-1 cells (2.5×10^5) prelabeled with Alexa564-conjugated concanavalin A were added to the culture. Cells were then allowed to adhere for 30 min on a rocking platform. After two washes with phosphate-buffered saline, fluorescent images were immediately obtained by a fluorescent microscope IX71 with DP70 image capture (Olympus) and processed using Adobe Photoshop, version 7.0. Adhesion of red fluorescent cells was quantified in three fields per well. Results are representative of three separate experiments and expressed as means ± S.D.

Immunofluorescence of VWF—Confluent HAECs were treated with 10 μg/ml LTA or 10 μM A23187 for 60 min. The culture media were removed, and the cells were immediately fixed at −20 °C with methanol for 60 min. Immunostaining was carried out using an anti-VWF rabbit polyclonal antibody (Santa Cruz Biotechnology, Santa Cruz, CA) and Alexa488-conjugated secondary antibody (Invitrogen). Cell nuclei were also stained with 2.5 μg/ml Höechst 33342 for 30 min. Images were obtained by a fluorescent microscope IX71 (magnification: ×40) with DP70 image capture (Olympus) in the presence of the Prolong Gold Antifade reagent (Invitrogen) and processed using Adobe Photoshop, version 7.0 (Adobe). Results are representative of three separate experiments.

Immunoblot Analysis—Confluent HAECs seeded on 60-mm plates were transfected with gene-specific siRNA and incubated in Opti-Mem I media containing 5% fetal bovine serum for 4–6 h. The cells were stimulated with 1 μg/ml LTA for 0–60 min and lysed with a buffer consisting of 20 mM Tris-hydrochloride (pH 7.2), 150 mM sodium chloride, 5 mM EDTA, and 1% Triton X-100 in the presence of protease inhibitors (Roche Applied Science) at 4 °C for 15 min followed by clarification by centrifugation at 12,000 × *g* for 10 min. SDS-PAGE and immunoblot analyses were performed as described previously (17, 20). Results are representative of three separate experiments.

Flow Cytometry—To assess the surface expression of P-selectin, confluent HAECs were treated with 10 μg/ml LTA for 30 min. To assess the surface expression of TLR2, confluent HAECs or HUVECs were treated with 10 ng/ml IFN-γ or they were incubated for 12 h under laminar flow. Cell culture under laminar flow was performed with a cone and plate apparatus as described previously (22). Magnitude of the flow was controlled at ~15 dyn/cm^2. The cells were then removed with phosphate-buffered saline containing 20 mM EDTA and fixed with phosphate-buffered saline containing 4% paraformaldehyde at 4 °C for 60 min. The cells were then incubated at 4 °C for 60 min with anti-TLR2 monoclonal antibody (IMG-319), anti-P-selectin monoclonal antibody (BD Biosciences), or isotype-matched mouse IgG and then with fluorescein isothiocyanate-conjugated anti-mouse IgG. Fluorescence was measured using a FACSCalibur (BD Biosciences).

Statistics—All values were evaluated by statistical analysis using one-way analysis of variance and Student-Newman-Keul's test. Differences were considered to be statistically significant at the level of $p < 0.05$.

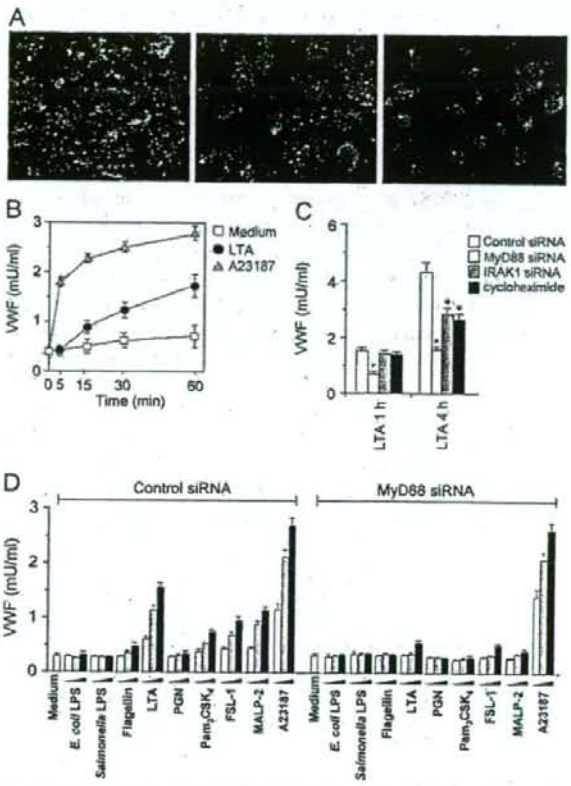

FIGURE 1. **MyD88-dependent Weibel-Palade body exocytosis by bacterial constituents.** *A*, HAECs stimulated with 10 μg/ml LTA or 1 μM A23187 for 60 min were fixed and stained immunofluorescently with anti-VWF antibody (*green*) and with Höechst33342 (*blue*). *Left*, unstimulated; *middle*, stimulated with LTA; *right*, stimulated with A23187. *B*, HAECs were stimulated with 1 μg/ml LTA or 1 μM A23187 for the indicated periods. The amounts of VWF released into the media were measured by ELISA. Each value is the mean ± S.D. ($n = 3$). *C*, HAECs transfected with MyD88 or IRAK1-specific or control siRNA were prepared. Cells were pretreated with 10 μg/ml cycloheximide for 30 min and then washed and stimulated with 10 μg/ml LTA for 60 min or 4 h. The amounts of VWF released into the media were measured by ELISA. Each value is the mean ± S.D. ($n = 3$). *, *versus* control group, $p < 0.01$. *D*, HAECs transfected with MyD88-specific or control siRNA were stimulated with *E. coli* LPS O26:B6 (0.01–1 μg/ml), LPS from *S. minnesota* (0.01–1 μg/ml), flagellin from *S. typhimurium* (0.1–10 μg/ml), LTA from *S. aureus* (0.1–10 μg/ml), PGN from *S. aureus* (0.1–10 μg/ml), Pam_3CSK_4 (0.1–10 μg/ml), FSL-1 (0.01–1 μg/ml), MALP-2 (0.01–1 μg/ml), and A23187 (0.1–10 μM) for 60 min, and then the amounts of VWF released into the media were measured. Each value is the mean ± S.D. ($n = 3$).

RESULTS

Induction of Weibel-Palade Body Exocytosis by Bacterial Constituents—We first examined whether bacterial LTA activated degranulation of Weibel-Palade bodies, because LTA has been reported to stimulate vascular endothelial cells, leading to induction of production of proinflammatory mediators, dysfunction, or cell death (23–25). After stimulation of HAECs for 30 min, LTA clearly decreased the amount of Weibel-Palade bodies, stained with an antibody to VWF, in the cells (Fig. 1*A*). Compared with the calcium ionophore (A23187)-induced response, we found that LTA gradually activated Weibel-Palade body exocytosis, quantification of which was performed by measuring the amount of VWF released into the media (Fig. 1*B*). VWF release by stimulation with

LTA for 60 min was not suppressed by treatment with the protein synthesis inhibitor cycloheximide, whereas the release by stimulation with LTA for 4 h was significantly suppressed by the treatment (Fig. 1*C*). We further investigated whether LTA induction of exocytosis was mediated through MyD88 and IRAK-1, common signaling molecules downstream of TLRs, because LTA is known as a TLR2 agonist. Interestingly, VWF release by stimulation with LTA for 60 min was suppressed by knockdown of the expression of MyD88 but not that of IRAK-1, whereas the release by stimulation with LTA for 4 h was significantly suppressed by each knockdown of MyD88 and IRAK-1 (Fig. 1*C*). Thus, these results suggest that LTA can induce Weibel-Palade body exocytosis through a MyD88-dependent rapid mechanism without *de novo* protein synthesis and an IRAK-1-dependent slower mechanism with *de novo* protein synthesis.

We also examined whether other bacterial cell wall constituents, as shown in Table 1, activated induction of VWF release after stimulation of HAECs for 60 min. Among the compounds that we tested, the synthetic analogs of bacterial lipoproteins Pam_3CSK_4, FSL-1, and MALP-2 and, to a lesser extent, flagellin induced VWF release in a dose-dependent manner (Fig. 1*D*, *left*). Interestingly, LPS from different bacterial species and PGN did not activate Weibel-Palade body exocytosis (Fig. 1*D*, *left*). In addition, we found that induction of exocytosis by bacterial compounds was also mediated by MyD88 as well as that by LTA (Fig. 1*D*, *right*). These results suggest that several types of, but not all, bacterial cell wall constituents can activate induction of TLR-MyD88-mediated exocytosis.

TABLE 1
Bacterial cell wall constituents used in this study

Substance	Origin (Ref.)	TLR recognition in human cells (Ref.)
LTA	*S. aureus*	TLR2 (7)
LPS	*E. coli*	TLR4 (10)
LPS	*S. minnesota*	TLR4 (10)
Flagellin	*S. typhimurium*	TLR5 (9)
PGN	*S. aureus*	TLR2 (8)
Pam_3CSK_4	Synthesis (*E. coli*) (16)	TLR1/TLR2 (41)
FSL-1	Synthesis (*M. salivarium*) (18)	TLR2/TLR6 (17)
MALP-2	Synthesis (*M. fermentans*) (19)	TLR2/TLR6 (55)

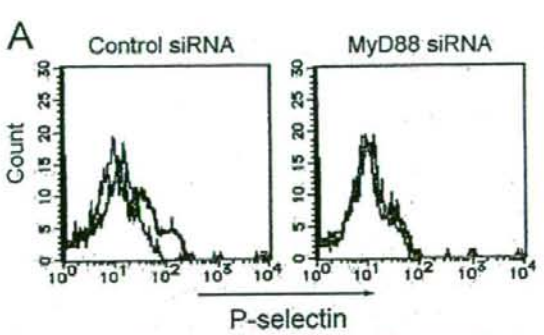

FIGURE 2. **MyD88-dependent P-selectin externalization by LTA.** *A*, HAECs transfected with MyD88-specific or control siRNA were stimulated with 10 μg/ml LTA for 60 min, and then surface P-selectin was detected by flow cytometry. *Shaded histogram*, not stimulated; *gray*, stimulated with LTA. *B*, HAECs transfected with MyD88-specific or control siRNA were stimulated with 10 μg/ml LTA for 60 min, and monocytes stained with conA-Alexa594 were then allowed to adhere for 20 min. Adhesion of red fluorescent cells was quantified in three fields per well by using an image analysis system. Each value is the mean ± S.D. ($n = 3$). *, $p < 0.01$.

Regarding the process of Weibel-Palade body exocyt found that MyD88-dependent externalization of P-selec induced after stimulation of HAECs with LTA for 30 m 2*A*). In addition, monocyte adhesion to HAECs was m increased in a MyD88-dependent fashion after LTA s tion for 60 min (Fig. 2*B*).

Stimulatory Activities of LPS and PGN in HAECs—A above, LPS did not activate Weibel-Palade body exocyto 1*D*). However, LPS potently activated induction of My pendent IL-8 production in HAECs after stimulation for 3*A*). Thus, the results shown in Figs. 1*D* and 3*A* suggest th thelial TLR4 lacks the ability to induce rapid Weibel-Pala exocytosis without *de novo* protein synthesis. Similarly PGN did not activate Weibel-Palade body exocytosis (Also, PGN did not induce IL-8 production after stimulatio in HAECs, whereas LTA did (Fig. 3*A*). However, our pre of PGN had activities to induce TNF-α production in monocytes (Fig. 3*B*) and TLR2- and MyD88-dependent a of NF-κB in HEK293 cells (Fig. 3*C*) in a way similar to th case of other TLR2 agonists. These results suggest that lack the ability to respond to PGN.

Induction of Weibel-Palade Body Exocytosis through We then focused on LTA- and bacterial lipopeptide- Weibel-Palade body exocytosis. It has been reported t and bacterial lipopeptides are TLR2 agonists (Tabl HUVECs, the lipopeptide FSL-1 induced VWF release (We found that this response was enhanced by increased sion of TLR2 by gene transfection (Fig. 4*A*). This result that TLR2 recognition of bacterial constituents direc vates Weibel-Palade body exocytosis. Moreover, transfe mutated TLR2 (P681H), which lacks the ability to inter MyD88 (26), suppressed the release (Fig. 4*B*), consist the results presented in Figs. 1*D* and 2*A* showing that was involved in the induction of Weibel-Palade exocy HAECs, knockdown of TLR2 expression resulted in complete suppression of VWF release by Pam_3CSK_4 MALP-2, and LTA (Fig. 4*B*). Moreover, knockdown expression resulted in a decrease in the activities of LTA and MALP-2 and even that of Pam_3CSK_4 (Fig. 4*B*). In to this, TLR1 interference did not affect VWF release (consistent with our observa HAECs express very low TLR1 mRNA compared v levels of TLR2 mRNA (d shown). These results sugg endothelial recognition of gens by TLR2, or to a lesse by TLR6, contributes to in of Weibel-Palade body exoc

Involvement of PLCγ Ac in Weibel-Palade Body Exo Recent studies have sho TLR2 signal transduction r an increase of intracellular level (27, 28). Indeed, we fo the intracellular calcium BAPTA-AM suppressed duced exocytosis (Fig. 5

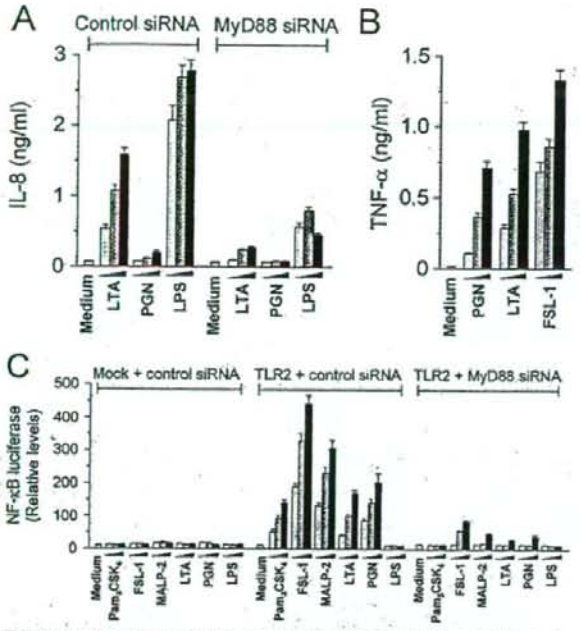

FIGURE 3. **Stimulatory activities of LPS and PGN in HAECs.** *A*, HAECs transfected with MyD88-specific or control siRNA were stimulated with LTA (0.1–10 μg/ml), PGN (0.1–10 μg/ml), and LPS (1–100 ng/ml) for 4 h, and then the amounts of IL-8 released into the media were measured. Each value is the mean ± S.D. ($n = 3$). *B*, THP-1 cells were stimulated with PGN (0.1–10 μg/ml), LTA (0.1–10 μg/ml), and FSL-1 (10–1 μg/ml) for 6 h, and then the amounts of TNF-α released into the media were measured. Each value is the mean ± S.D. ($n = 3$). *C*, HEK293 cells stably expressing TLR2, and control cells were prepared and then transfected with MyD88-specific siRNA and NF-κB-driven luciferase gene. The cells were stimulated with Pam_3CSK_4 (0.1–10 μg/ml), FSL-1 (0.01–1 μg/ml), MALP-2 (0.01–1 μg/ml), LTA (0.1–10 μg/ml), PGN (0.1–10 μg/ml), and LPS (1–100 ng/ml) for 6 h, and then luciferase activity was measured. Each value is the mean ± S.D. ($n = 3$).

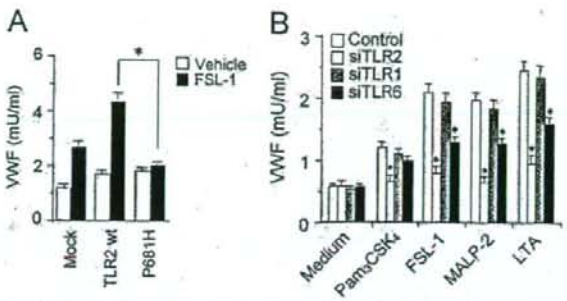

FIGURE 4. **Involvement of TLR2 in Weibel-Palade body exocytosis.** *A*, HUVECs transfected with WT or P681H mutant of TLR2 or with a control plasmid were stimulated with 1 μg/ml FSL-1 for 60 min, and then the amounts of VWF released into the media were measured. Each value is the mean ± S.D. ($n = 3$). *B*, HAECs transfected with TLR1-, TLR2-, or TLR6-specific or control siRNA were stimulated with Pam_3CSK_4 (10 μg/ml), FSL-1 (1 μg/ml), MALP-2 (1 μg/ml), and LTA (10 μg/ml) for 60 min, and then the amounts of VWF released into the media were measured. Each value is the mean ± S.D. ($n = 3$). *, $p < 0.05$.

therefore examined the role of PLCγ, a common regulator of intracellular calcium release by generating inositol 1,4,5-triphosphate (29), during TLR2-mediated Weibel-Palade body exocytosis. We found that the PLCγ inhibitor U-73122 significantly suppressed TLR2 agonist-induced VWF release (Fig. 5*B*). Because PLCγ isoforms are thought to be activated by phosphatidylinositol 3,4,5-trisphosphate, the product of phosphatidylinositol 3-kinases (PI3Ks) (29), TLR2-mediated exocytosis was suppressed by the chemical inhibitor of PI3K LY294002 (data not shown). However, downstream of TLR/IL-1R, activation of PI3K is regulated through a MyD88-independent machinery (30), conflicting with our results showing that Weibel-Palade body exocytosis requires MyD88 (Figs. 1*D* and 2*A*). Because enzymatic activity of PLCγ is also regulated by tyrosine phosphorylation (31), we tested whether this event was mediated by MyD88. Phosphorylation of PLCγ1 at the Tyr-738 residue was induced by LTA stimulation (Fig. 5*C*). Interestingly, this activity was efficiently suppressed by knockdown of MyD88 expression but not by knockdown of IRAK-1 expression (Fig. 5*C*). MyD88-dependent activation of PLCγ was also observed in TLR2-overexpressed 293 cells used as non-endothelial cells (data not shown). These results suggest that TLR2-mediated rapid Weibel-Palade body exocytosis is regulated by activation of PLCγ through MyD88-dependent tyrosine phosphorylation.

We also investigated the role of PLCγ in TLR2-mediated NF-κB signaling. U-73122 treatment clearly suppressed TLR2 agonist-induced production of the NF-κB-driven chemokine IL-8 in HAECs (Fig. 5*D*). U-73122 treatment also suppressed LTA-induced phosphorylation and degradation of IκBα in HAECs (Fig. 5*E*). These results suggest that the MyD88-PLCγ pathway also mediates inflammatory responses through NF-κB activation in endothelial cells.

Regulation of TLR2-mediated Weibel-Palade Body Exocytosis—The results shown in Fig. 4 (*A* and *B*) raised the possibility that alteration of endothelial TLR2 expression affects the magnitude of Weibel-Palade body exocytosis. We examined TLR2-mediated exocytosis in the presence of vascular modulators, IFN-γ or laminar flow, which are known to affect TLR2 expression in endothelial cells of human origin. Consistent with the results of a previous study (32), treatment with IFN-γ increased TLR2 expression level in HAECs (Fig. 6*A*). Under this condition, the magnitude of TLR2-mediated exocytosis was significantly increased (Fig. 6*B*). In contrast to this, TLR2 expression slightly decreased in HAECs incubated under laminar flow (Fig. 6*C*), consistent with the results of a previous study (33). We found that laminar flow decreased the magnitude of TLR2-mediated exocytosis (Fig. 6*D*).

DISCUSSION

The major finding of this study is that aortic endothelial cells respond to several bacterial constituents that stimulate TLR2, leading to induction of Weibel-Palade body exocytosis through a MyD88-dependent mechanism without *de novo* protein synthesis. During this process, release of VWF and externalization of P-selectin were induced, by which rolling and adhesion of platelets and leukocytes and thrombus formation in the local vessel walls may be promoted (34, 35). The pathological role of this phenomenon *in vivo* may be support by the observations in mouse experiments, *i.e.* slight increases of local leukocyte-endothelial interaction after LTA administration (36) and soluble P-selectin level in serum after administration of the synthetic

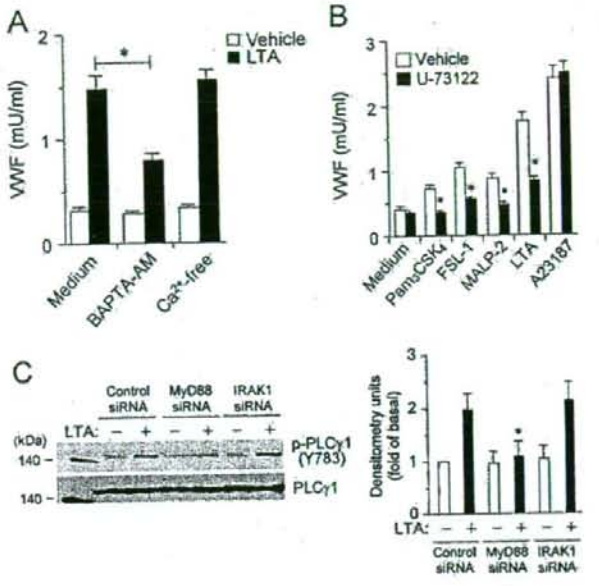

FIGURE 5. **PLCγ-mediation of TLR2-activated Weibel-Palade body exocytosis and NF-κB activation.** *A*, confluent HAECs were pretreated with 20 μM BAPTA-AM for 30 min or incubated in Ca^{2+}-free media. Then the cells were washed and stimulated with 10 μg/ml LTA for 60 min in Ca^{2+}-free media. The amounts of VWF released into the media were measured by ELISA. Each value is the mean ± S.D. ($n = 3$). *, $p < 0.01$. *B*, HAECs were pretreated with 10 μM U-73122 for 30 min and then washed and stimulated with Pam_3CSK_4 (10 μg/ml), FSL-1 (1 μg/ml), MALP-2 (1 μg/ml), LTA (10 μg/ml), and A23187 (1 μM) for 60 min. The amounts of VWF released into the media were measured by ELISA. Each value is the mean ± S.D. ($n = 3$). *, *versus* vehicle group, $p < 0.01$. *C*, HAECs transfected with MyD88- or IRAK1-specific or control siRNA were stimulated with 10 μg/ml LTA for 90 min. Immunoblot analysis was then performed to examine the expression of phosphorylated PLCγ1 (Y783) and total PLCγ1 (*left*). Immunoreactive bands were quantified by a densitometer (*right*). Results are expressed as means ± S.D. of three independent experiments. *, *versus* control group, $p < 0.01$. *D*, HAECs were pretreated with 10 μM U73122 for 30 min and then washed and stimulated with Pam_3CSK_4 (10 μg/ml), FSL-1 (1 μg/ml), MALP-2 (1 μg/ml), LTA (10 μg/ml), and A23187 (1 μM) for 4 h. The amounts of IL-8 released into the media were measured by ELISA. Each value is the mean ± S.D. ($n = 3$). *, *versus* vehicle group, $p < 0.01$. *E*, HAECs were pretreated with 10 μM U73122 for 30 min and then washed and stimulated with 10 μg/ml LTA for the indicated period. Immunoblot analysis was then performed to examine the expression of IκBα and glyceraldehyde-3-phosphate dehydrogenase (*GAPDH*).

lipopeptide FSL-1.[3] Sequentially or simultaneously, both PLCγ- and IRAK1-mediated signaling pathways activate NF-κB, by which production of various proinflammatory cyto-

[3] T. Into, Y. Kanno, J.-I. Dohkan, M. Nakashima, M. Inomata, K.-I. Shibata, C. J. Lowenstein, and K. Katsushita, unpublished data.

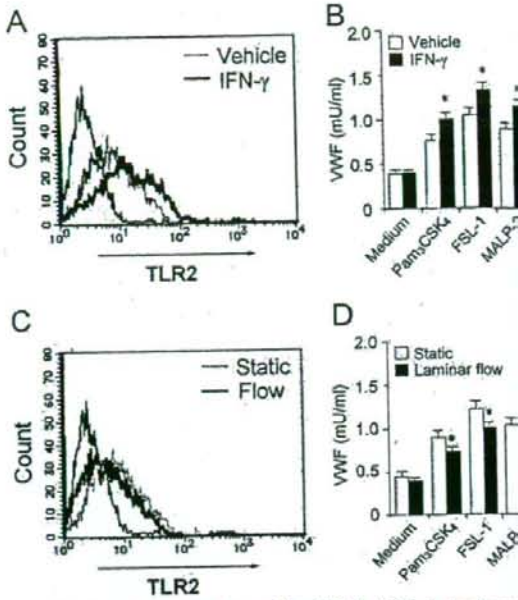

FIGURE 6. **Regulation of TLR2-mediated Weibel-Palade body exo** *A* and *B*, HAECs were treated with IFN-γ for 12 h. Surface TLR2 expres detected by flow cytometry (*A*). The *shaded histogram* indicates cell with control antibody. The cells were washed and stimulated with P (10 μg/ml), FSL-1 (1 μg/ml), MALP-2 (1 μg/ml), and LTA (10 μg/ml) fo The amounts of VWF released into the media were measured by Each value is the mean ± S.D. ($n = 3$). *, *versus* vehicle group, $p < 0.$ *D*, HAECs were incubated under laminar flow for 12 h. Surface TLR sion was detected by flow cytometry (*C*). The *shaded histogram* indic stained with control antibody. The cells were then stimulated with P (10 μg/ml), FSL-1 (1 μg/ml), MALP-2 (1 μg/ml), and LTA (10 μg/ml) fo The amounts of VWF released into the media were measured by Each value is the mean ± S.D. ($n = 3$). *, *versus* static group, $p < 0.0$

kines, and expression of adhesion molecules such as I are induced to promote adherence and activation of p and leukocytes (37). The delayed Weibel-Palade body e sis with *de novo* protein synthesis is further activate cells. Therefore, endothelial TLR2 may be able to funct primary initiator and a modulator of artery inflam through these early-phase endothelial responses after r tion of cognate agonists.

We investigated the responsiveness of HAECs towa mon bacterial constituents. For the TLR2 agonists, we p several compounds that have already been proposed tion as TLR2 agonists, because TLR2 forms a complica ognition system and because human endothelial cells fi ferent vascular beds show different degrees of responsiv TLR2 agonists (32, 38, 39). Unexpectedly, PGN, unli TLR2 agonists, could not activate either Weibel-Pala exocytosis or IL-8 production (Figs. 1*D* and 3*A*). The recognition of PGN by TLR2 is still controversial. The e of an intracellular receptor for PGN (NOD2) further cates this matter. However, Gupta's group recently co that PGN is in fact recognized by TLR2 by showing th amidase treatment of PGN abolished the TLR2-stir activity (8). We showed that recognition of our PGN wa dependent on TLR2 (Fig. 3*A*). It has been shown th directly binds TLR2 *per se* (40), whereas bacterial lipo

are thought to directly interact with TLR2-associated molecules such as CD14 and LBP but not with TLR2 *per se* (7, 41, 42), suggesting the existence of different ligand-recognition mechanisms by TLR2. Furthermore, a novel family of PGN-binding proteins such as peptidoglycan recognition proteins has been found (43) and might enable discrimination of PGN from other TLR2 agonists. Thus, PGN may be recognized by a TLR2 recognition system different from that for LTA and lipoproteins/lipopeptides. Collectively, HAECs express functional TLR2 to respond to several TLR2 agonists, including lipopeptides and LTA, but may lack a PGN-recognition system resulting in an inability to respond to PGN. Moreover, aortic endothelial cells may particularly recognize diacylglyceride-containing bacterial lipid derivatives (LTA and bacterial lipopeptides), recognition of which has recently been reported to depend on TLR6 and CD36 (11).

We also showed that the TLR4 agonist LPS did not activate Weibel-Palade body exocytosis (Fig. 1*D*). Although the reason for this is not clear, several lines of evidence obtained in previous studies may provide an explanation. For example, TLR4 expression has been reported to localize intracellularly in artery endothelial cells (44). This observation suggests that TLR4 in artery endothelial cells may be lacking in induction of phospholipid-dependent signaling events, including PLCγ activation, which are commonly intrinsic to the signaling receptors spanning the cell membrane. Further investigation is needed to determine the reason.

Several properties of endothelial TLR2 have been proposed to be involved in the development of atherosclerosis. First, endothelial TLR2 expression is enhanced by proinflammatory stimuli, such as TNF-α, IFN-γ, and LPS (32), and by SP-1-dependent machinery in areas of disturbed blood flow such as lesion predilection within the aortic tree and heart (33). The expression level of TLR2 is indeed increased in an atherosclerotic lesion in humans (45). Furthermore, a recent study has revealed that complete deficiency of TLR2 in atherosclerosis-prone LDLR-null mice leads to an apparent reduction in the formation of lesions (46). Proinflammatory signaling pathways downstream of TLR2 have been thought to be activated through TIRAP/Mal, MyD88, IRAK-1, and TRAF6 in endothelial cells. Other pathways involving PI3K and the downstream protein kinase Akt/PKB (47), the Rho family GTPase Rac1 (48), and the redox-activated mitogen-activated protein kinase kinase kinase ASK1 (49) also link TLR2 signaling to the NF-κB pathway. In this study, we showed that PLCγ also mediated the NF-κB pathway downstream of TLR2 in HAECs, although involvement of PLCγ in the TLR2 proinflammatory signaling has been described in several reports (27, 50). Because PLCγ isoforms are thought to be activated by both generation of phosphatidylinositol 3,4,5-triphosphate by PI3K and tyrosine phosphorylation, we found the latter process downstream of TLR2 was dependent on MyD88 but not IRAK-1 (Fig. 5*C*). Recent studies have suggested a linkage of TLRs and tyrosine kinases, including Syk via MyD88-STAP-2 interaction (51) and Btk via direct interaction with TIR domain (52), both of which have been shown to activate PLCγ isoforms. Moreover, Btk-induced phosphorylation of TIRAP/Mal has recently been reported to play an important role in TLR signal transduction

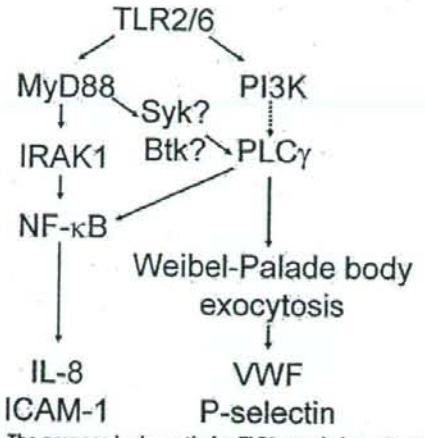

FIGURE 7. **The proposed schematic for TLR2 regulation of early-phase inflammatory signaling in human aortic endothelial cells.**

(53), which may occur at a phosphatidylinositol diphosphate-rich membrane compartment after recruitment of MyD88 to membrane-localized TIRAP/Mal (54). A schematic of signaling pathways proposed here is shown in Fig. 7.

Endothelial activation by several proinflammatory agents has been shown to increase endothelial responsiveness toward TLR2 agonists via up-regulation of TLR2 expression (32). Increased endothelial TLR2 expression increased the magnitude of TLR2-mediated exocytosis of Weibel-Palade bodies (Fig. 6*B*) and endothelial responses (38), suggesting enhanced responsiveness of endothelial cells to pathogens in inflamed lesions. In contrast, fluid shear decreased the magnitude of TLR2 ligand-stimulated Weibel-Palade body exocytosis (Fig. 6*D*). Physiological fluid shear stress has been suggested to have atheroprotective effects *in vivo*, because atherosclerosis preferentially occurs in an area of disturbed flow or a low level of shear stress, whereas regions with steady laminar flow and physiological shear stress are protected. Disturbed flow or a low level of shear stress has been reported to regulate expression of various regulatory molecules of endothelial activation, by which atherosclerotic processes may be accelerated in the sites. These observations are consistent with the previous finding that physiological fluid shear stress decreases endothelial TLR2 expression via impaired activity of the transcriptional factor SP1 (33). Thus, our results raise the possibility that bacterial constituent-induced Weibel-Palade body exocytosis can be physiologically or pathologically regulated in particular circumstances of the vessel wall.

In conclusion, our study focused on endothelial exocytosis induced by bacterial pathogens and showed a linkage between endothelial innate recognition of pathogens and early-phase endothelial inflammatory responses. Our results may provide a new insight into the role of endothelial TLR2 in the initiation and modulation of vascular inflammation or atherogenic responses.

REFERENCES

1. Lowenstein, C. J., Morrell, C. N., and Yamakuchi, M. (2005) *Trends Cardiovasc. Med.* 15, 302–308
2. Rondaij, M. G., Bierings, R., Kragt, A., van Mourik, J. A., and Voorberg, J.

(2006) *Arterioscler. Thromb. Vasc. Biol.* **26,** 1002–1007
3. Danesh, J. (1999) *Am. Heart J.* **138,** S434–S437
4. Desvarieux, M., Demmer, R. T., Rundek, T., Boden-Albala, B., Jacobs, D. R., Jr., Sacco, R. L., and Papapanou, P. N. (2005) *Circulation* **111,** 576–582
5. Akira, S., and Takeda, K. (2004) *Nat. Rev. Immunol.* **4,** 499–511
6. Kirschning, C. J., and Schumann, R. R. (2002) *Curr. Top. Microbiol. Immunol.* **270,** 121–144
7. Schroder, N. W., Morath, S., Alexander, C., Hamann, L., Hartung, T., Zahringer, U., Gobel, U. B., Weber, J. R., and Schumann, R. R. (2003) *J. Biol. Chem.* **278,** 15587–15594
8. Dziarski, R., and Gupta, D. (2005) *Infect. Immun.* **73,** 5212–5216
9. Reed, K. A., Hobert, M. E., Kolenda, C. E., Sands, K. A., Rathman, M., O'Connor, M., Lyons, S., Gewirtz, A. T., Sansonetti, P. J., and Madara, J. L. (2002) *J. Biol. Chem.* **277,** 13346–13353
10. Tapping, R. I., Akashi, S., Miyake, K., Godowski, P. J., and Tobias, P. S. (2000) *J. Immunol.* **165,** 5780–5787
11. Hoebe, K., Georgel, P., Rutschmann, S., Du, X., Mudd, S., Crozat, K., Sovath, S., Shamel, L., Hartung, T., Zahringer, U., and Beutler, B. (2005) *Nature* **433,** 523–527
12. Jeannin, P., Bottazzi, B., Sironi, M., Doni, A., Rusnati, M., Presta, M., Maina, V., Magistrelli, G., Haeuw, J. F., Hoeffel, G., Thieblemont, N., Corvaia, N., Garlanda, C., Delneste, Y., and Mantovani, A. (2005) *Immunity* **22,** 551–560
13. Mullaly, S. C., and Kubes, P. (2004) *Circ. Res.* **95,** 657–659
14. Tobias, P., and Curtiss, L. K. (2005) *J. Lipid Res.* **46,** 404–411
15. Michelsen, K. S., Doherty, T. M., Shah, P. K., and Arditi, M. (2004) *J. Immunol.* **173,** 5901–5907
16. Hoffmann, P., Heinle, S., Schade, U. F., Loppnow, H., Ulmer, A. J., Flad, H. D., Jung, G., and Bessler, W. G. (1988) *Immunobiology* **177,** 158–170
17. Fujita, M., Into, T., Yasuda, M., Okusawa, T., Hamahira, S., Kuroki, Y., Eto, A., Nisizawa, T., Morita, M., and Shibata, K. (2003) *J. Immunol.* **171,** 3675–3683
18. Shibata, K., Hasebe, A., Into, T., Yamada, M., and Watanabe, T. (2000) *J. Immunol.* **165,** 6538–6544
19. Muhlradt, P. F., Kiess, M., Meyer, H., Sussmuth, R., and Jung, G. (1997) *J. Exp. Med.* **185,** 1951–1958
20. Into, T., Kiura, K., Yasuda, M., Kataoka, H., Inoue, N., Hasebe, A., Takeda, K., Akira, S., and Shibata, K. (2004) *Cell Microbiol.* **6,** 187–199
21. Matsushita, K., Morrell, C. N., Cambien, B., Yang, S. X., Yamakuchi, M., Bao, C., Hara, M. R., Quick, R. A., Cao, W., O'Rourke, B., Lowenstein, J. M., Pevsner, J., Wagner, D. D., and Lowenstein, C. J. (2003) *Cell* **115,** 139–150
22. Dimmeler, S., Haendeler, J., Rippmann, V., Nehls, M., and Zeiher, A. M. (1996) *FEBS Lett.* **399,** 71–74
23. Doran, K. S., Engelson, E. J., Khosravi, A., Maisey, H. C., Fedtke, I., Equils, O., Michelsen, K. S., Arditi, M., Peschel, A., and Nizet, V. (2005) *J. Clin. Invest.* **115,** 2499–2507
24. Bermpohl, D., Halle, A., Freyer, D., Dagand, E., Braun, J. S., Bechmann, I., Schroder, N. W., and Weber, J. R. (2005) *J. Clin. Invest.* **115,** 1607–1615
25. Talreja, J., Kabir, M. H., Filla, M. B., Stechschulte, D. J., and Dileepan, K. N. (2004) *Immunology* **113,** 224–233
26. Xu, Y., Tao, X., Shen, B., Horng, T., Medzhitov, R., Manley, J. L., and Tong, L. (2000) *Nature* **408,** 111–115
27. Chun, J., and Prince, A. (2006) *J. Immunol.* **177,** 1330–1337
28. Supajatura, V., Ushio, H., Nakao, A., Akira, S., Okumura, K., Ra, C., and Ogawa, H. (2002) *J. Clin. Invest.* **109,** 1351–1359
29. Bae, Y. S., Cantley, L. G., Chen, C. S., Kim, S. R., Kwon, K. S., and Rhee, S. G. (1998) *J. Biol. Chem.* **273,** 4465–4469
30. Davis, C. N., Mann, E., Behrens, M. M., Gaidarova, S., Rebek, M., R Jr., and Bartfai, T. (2006) *Proc. Natl. Acad. Sci. U. S. A.* **103,** 2953–
31. Law, C. L., Chandran, K. A., Sidorenko, S. P., and Clark, E. A. (199 *Cell Biol.* **16,** 1305–1315
32. Faure, E., Thomas, L., Xu, H., Medvedev, A., Equils, O., and Ar (2001) *J. Immunol.* **166,** 2018–2024
33. Dunzendorfer, S., Lee, H. K., and Tobias, P. S. (2004) *Circ.* 684–691
34. Andre, P., Denis, C. V., Ware, J., Saffaripour, S., Hynes, R. O., Z. M., and Wagner, D. D. (2000) *Blood* **96,** 3322–3328
35. Massberg, S., Brand, K., Gruner, S., Page, S., Muller, E., Muller, meier, W., Richter, T., Lorenz, M., Konrad, I., Nieswandt, B., and M. (2002) *J. Exp. Med.* **196,** 887–896
36. Yipp, B. G., Andonegui, G., Howlett, C. J., Robbins, S. M., Hartung M., and Kubes, P. (2002) *J. Immunol.* **168,** 4650–4658
37. Collins, T., Read, M. A., Neish, A. S., Whitley, M. Z., Thanos, Maniatis, T. (1995) *FASEB J.* **9,** 899–909
38. Bulut, Y., Faure, E., Thomas, L., Equils, O., and Arditi, M. (2001) *J. I* **167,** 987–994
39. Faure, E., Equils, O., Sieling, P. A., Thomas, L., Zhang, F. X., Kir C. J., Polentarutti, N., Muzio, M., and Arditi, M. (2000) *J. Biol. Ch* 11058–11063
40. Iwaki, D., Mitsuzawa, H., Murakami, S., Sano, H., Konishi, M., A and Kuroki, Y. (2002) *J. Biol. Chem.* **277,** 24315–24320
41. Manukyan, M., Triantafilou, K., Triantafilou, M., Mackie, A., Ni Espevik, T., Wiesmuller, K. H., Ulmer, A. J., and Heine, H. (20 *J. Immunol.* **35,** 911–921
42. Schroder, N. W., Heine, H., Alexander, C., Manukyan, M., E Hamann, L., Gobel, U. B., and Schumann, R. R. (2004) *J. Immu* 2683–2691
43. Dziarski, R., and Gupta, D. (2006) *Cell Microbiol.* **8,** 1059–1069
44. Dunzendorfer, S., Lee, H. K., Soldau, K., and Tobias, P. S. (2004) **18,** 1117–1119
45. Edfeldt, K., Swedenborg, J., Hansson, G. K., and Yan, Z. Q *Circulation* **105,** 1158–1161
46. Mullick, A. E., Tobias, P. S., and Curtiss, L. K. (2005) *J. Clin. Inv* 3149–3156
47. Martin, M., Schifferle, R. E., Cuesta, N., Vogel, S. N., Katz, J., and N S. M. (2003) *J. Immunol.* **171,** 717–725
48. Arbibe, L., Mira, J. P., Teusch, N., Kline, L., Guha, M., Mack Godowski, P. J., Ulevitch, R. J., and Knaus, U. G. (2000) *Nat. Imm* 533–540
49. Into, T., and Shibata, K. (2005) *Cell Microbiol.* **7,** 1305–1317
50. Lee, C. W., Chien, C. S., and Yang, C. M. (2004) *Am. J. Phys* L921–L930
51. Sekine, Y., Yumioka, T., Yamamoto, T., Muromoto, R., Imoto, S., K., Oritani, K., Shimoda, K., Minoguchi, M., Akira, S., Yoshimura Matsuda, T. (2006) *J. Immunol.* **176,** 380–389
52. Horwood, N. J., Page, T. H., McDaid, J. P., Palmer, C. D., Can Mahon, T., Brennan, F. M., Webster, D., and Foxwell, B. M *J. Immunol.* **176,** 3635–3641
53. Gray, P., Dunne, A., Brikos, C., Jefferies, C. A., Doyle, S. L., and L. A. (2006) *J. Biol. Chem.* **281,** 10489–10495
54. Kagan, J. C., and Medzhitov, R. (2006) *Cell* **125,** 943–955
55. Nakao, Y., Funami, K., Kikkawa, S., Taniguchi, M., Nishiguchi, M mori, Y., Seya, T., and Matsumoto, M. (2005) *J. Immunol.* **174,** 15

Biochem. J. (2007) 405, 69–75 (Printed in Great Britain) doi:10.1042/BJ20070104

Runx3 negatively regulates Osterix expression in dental pulp cells

Li ZHENG*, Koichiro IOHARA*, Masaki ISHIKAWA†, Takeshi INTO*, Teruko TAKANO-YAMAMOTO‡, Kenji MATSUSHITA* and Misako NAKASHIMA*[1]

*Laboratory of Oral Disease Research, National Institute for Longevity Sciences, National Center for Geriatrics and Gerontology, Aichi 474-8522, Japan, †Department of Endodontology and Operative Dentistry, Division of Oral Rehabilitation, Faculty of Dental Science, Kyushu University, Fukuoka 812-8582, Japan, and ‡Division of Orthodontics and Dentofacial Orthopedics, Graduate School of Dentistry, Tohoku University, Sendai 980-8575, Japan

Osterix, a zinc-finger-containing transcription factor, is required for osteoblast differentiation and bone formation. *Osterix* is also expressed in dental mesenchymal cells of the tooth germ. However, transcriptional regulation by Osterix in tooth development is not clear. Genetic studies in osteogenesis place *Osterix* downstream of Runx2 (Runt-related 2). The expression of *Osterix* in odontoblasts overlaps with Runx3 during terminal differentiation *in vivo*. Runx3 down-regulates *Osterix* expression in mouse DPCs (dental pulp cells). Therefore the regulatory role of Runx3 on *Osterix* expression in tooth development was investigated. Enforced expression of Runx3 down-regulated the activity of the *Osterix* promoter in the human embryonic kidney 293 cell line. When the Runx3 responsive element on the *Osterix* promoter, located at −713 to −707 bp (site 3, AGTGGTT) relative to the cap site, was mutated, this down-regulation was abrogated. Furthermore, electrophoretic mobility-shift assay and chromatin immunoprecipitation assays in mouse DPCs demonstrated direct functional binding of Runx3 to the *Osterix* promoter. These results demonstrate the transcriptional regulation of *Osterix* expression by Runx3 during differentiation of dental pulp cells into odontoblasts during tooth development.

Key words: bone morphogenetic protein 2 (BMP2), dental pulp cell (DPC), Osterix, Runx2, Runx3, tooth development.

INTRODUCTION

The transcriptional regulation of cell proliferation and differentiation by the Runx (Runt-related) family of DNA-binding transcription factors is critical for both morphogenesis and regeneration. The regulatory function of the Runx family on the promoters and enhancers of target genes, where they associate with cofactors and other DNA-binding transcription factors to modulate gene expression, is well known [1]. The Runx family is composed of three members designated Runx1 (AML1/Cbfα2), Runx2 (AML2/Cbfα1) and Runx3 (AML3/Cbfα3) [2,3]. Although the Runx members share highly conserved DNA-binding domains, they regulate distinct functions [4–7]. Runx1 is involved in the regulation of haematopoiesis [8], Runx2 is essential for bone and tooth development [9–11], and Runx3 is critical for gastric epithelial differentiation, neurogenesis of the dorsal root ganglia and T cell differentiation [8–10,12–16].

Stringent control of gene activation and suppression is required for tooth development. The optimal gene expression during dentin formation is dependent on integration and regulation of signals that govern the commitment of stem/progenitor cells into the pulp cell lineage, and their subsequent proliferation and differentiation into odontoblasts. Runx2 is essential for tooth formation. Molar development is arrested at the late bud stage in Runx2 homozygous mice [11], correlating with the intense expression of Runx2 in the dental mesenchyme during the bud and cap stages [17]. Runx3 is co-expressed in dental papillae at the cap and early bell stages, along with Runx2. Later Runx3 is restricted to the odontoblastic layer at the late bell stage, while Runx2 is no longer detected [17]. Runx proteins might play a pivotal role in governing the control of the physiological response of dental genes.

Osterix, a zinc-finger-containing transcription factor, is required for osteoblast differentiation and bone formation [18]. In *Osterix* null mice, no bone formation occurs, similar to the phenotypes in *Runx2* null mice [9,18]. However, Runx2 is expressed without major alterations in *Osterix* null mice. In contrast, Osterix is not expressed in *Runx2* null mice, demonstrating that Osterix acts downstream of Runx2 [18]. Transcriptional regulation of *Osterix* by Runx2 in cartilage has been suggested recently [19]. In addition, *Osterix* expression has been observed in mesenchymal cells of the tooth germ [18]. The expression of *Osterix* and its transcriptional regulation by Runx proteins during tooth development have not been investigated.

In the present study, we investigated the expression of *Osterix* during tooth development, and demonstrate that *Osterix* is expressed strictly in the odontoblastic layer at the bell and the differentiation stages, overlapping with *Runx3*. Therefore the regulation of the expression of *Osterix* by Runx3 was examined further. Our results demonstrate that Runx3 binds directly to the *Osterix* promoter and down-regulates its expression in DPCs (dental pulp cells).

EXPERIMENTAL

Cloning of the *Osterix* promoter

To clone the Osterix promoter (nucleotides 66 to 1751; GenBank accession no. DQ229136), genomic DNA was isolated from the tail of an ICR mouse. PCR was performed using two primers: Osterix promoter 5′-1, 5′-TCTGTCCCTCAGTCCTGCTT-3′ and Osterix promoter 3′-2, 5-GGGCAAGTTGTCAGAGCTTC-3′. The approx. 1.7 kbp PCR product was then subcloned into MluI

Abbreviations used: BMP, bone morphogenetic protein; ChIP, chromatin immunoprecipitation; DIG, digoxigenin; DMEM, Dulbecco's modified Eagle's medium; DPC, dental pulp cell; Dspp, dentin sialophosphoprotein; DTT, dithiothreitol; EGFP, enhanced green fluorescent protein; EMSA, electrophoretic mobility-shift assay; FBS, foetal bovine serum; HEK-293, human embryonic kidney 293; KLK4, kallikrein 4; MSCV, murine stem cell virus; P1, postnatal day 1; RT, reverse transcription; Runx, Runt-related.

[1] To whom correspondence should be addressed (email misako@nils.go.jp).

and XhoI digested pGL3-promoter vector (Promega, Madison, WI, U.S.A.), and named pOsx1.7-luc. To prepare the MSCV (murine stem cell virus)-EGFP (enhanced green fluorescent protein)-FLAG-Runx3 expression vector, the following primers were used: FLAG-Runx3-5′, 5′-GGCAGATCTGCCACCATGGACTACAAGGACGATGACGACAAGGCTTCCAACAGCATCTTTG-3′ and Flag-Runx3-3′, 5′-ATATGAGCTCTCCCGCGTGGT-3′ to generate a Runx3 fragment with FLAG motif at N-terminal. The 300 bp PCR product was cloned in between the BglII and SacI sites in the pSL1180 vector (GE Healthcare, Buckinghamshire, U.K.) and named Flag-Runx3-300 bp-pSL1180. A 1.0 kbp Runx3 fragment was digested with SacI from the MSCV-EGFP-Runx3 plasmid (kindly provided by Dr Taniuchi Ichiro, Laboratory of Transcriptional Regulation, RIKEN Research Centre for Allergy and Immunology, Yokohama, Japan) and subcloned into the FLAG-Runx3-300 bp-pSL1180 vector to give FLAG-Runx3-pSL1180. The N-terminally FLAG-tagged full-length 1.3 kbp Runx3 was digested with BglII from FLAG-Runx3-pSL1180 and subcloned into the MSCV-EGFP vector, named MSCV-EGFP-FLAG-Runx3. The orientation of the inserts was confirmed by sequencing.

Site-directed mutagenesis

Three putative Runx2-binding sequences at positions −1823 to −1817 bp, −1776 to −1771 bp and −713 to −707 bp relative to the Cap site [19] were mutated using the QuikChange® Site-Directed Mutagenesis Kit (Stratagene, La Jolla, CA, U.S.A.) according to the manufacturer's recommendations. We generated mutants as follows; 5′-AACCACA-3′ at −1823/−1817 bp was changed into 5′-**GAGCTCA**-3′, 5′-ACCACT-3′ at −1776/−1771 bp was changed into 5′-**GCTACT**-3′ and 5′-AGTGGTT-3′ at −713/−707 bp was changed into 5′-**ATAGACT**-3′. The mutated nucleotides are indicated in bold. Mutations in single, double, and triple motifs were termed M1-M5 (Figure 3B). Incorporation of the mutated substitutions of all the constructs was confirmed by sequencing.

In situ hybridization

ICR mouse embryos at 15.0 days post coitum, 17.0 days post coitum and P1 (postnatal day 1) were fixed in 4% (w/v) paraformaldehyde at 4 °C overnight. *In situ* hybridization was carried out as described previously [20]. The following primers were used to amplify the mouse *Osterix* cDNA: Osterix-5′-1, 5′-GGTCCAGGCAACACACCTAC-3′ and Osterix-3′-2, 5′-GGTAGGGAGCTGGGTTAAGG-3′. The PCR product was ligated into the pBluescript II SK (−) vector (Stratagene). Mouse *Runx3* cDNA was removed from the MSCV-EGFP-Runx3 plasmid by digestion with EcoRI and then subcloned into the pBluescript II SK (−) vector. All inserts were confirmed by sequencing. The following cDNAs were used to generate sense (see Supplementary Figure 1 at http://www.BiochemJ.org/bj/405/bj4050069add.htm) and antisense riboprobes using either T3 or T7 RNA polymerase: a 184 bp murine Osterix fragment, a 1.2 kb Runx3 fragment and a 1.2 kb Bmp2 fragment. *In situ* hybridization was performed as described previously [21].

Cell culture and transfection studies

Mouse DPCs were isolated from tooth germ at 17.0 days post coitum. Mouse DPCs and HEK-293 (human embryonic kidney 293) cells were maintained in DMEM (Dulbecco's modified Eagle's medium) (Sigma, St. Louis, MO, U.S.A.) supplemented with 100 units/ml penicillin G, 100 μg/ml streptomycin (Invitrogen, Carlsbad, CA, U.S.A.) and 10% (v/v) FBS (foetal bovine serum; SAFC Biosciences, Lenexa, KS, U.S.A.). Experime assessing promoter activity by luciferase reporter gene express were performed as follows. HEK-293 cells (1×10^5) were pla in 24-well plates in serum-free DMEM without antibiotics 1 before use, and transiently transfected with 2 μg of the promo luciferase reporter gene plasmids, 3 μg of expression plasmid 0.2 μg of SV40 (simian virus 40) promoter construct (Prom as an internal standardized control for transfection efficie Transfections were performed using 2 μl/well of Lipofectamin 2000 (Invitrogen) following the manufacturer's instructions. MSCV-EGFP plasmid was also transfected as a control. A 4 h, the medium was replaced with DMEM supplemented 10% (v/v) FBS and cultured for an additional 44 h. Cells v then lysed, and luciferase activity was determined using a Luciferase Reporter Assay kit as instructed by the manufact (Promega). All activities were normalized against the co-tr fected internal control plasmid pRL-SV40 (Promega). For c expression experiments, 4×10^6 DPCs were transfected 8 μg of expression plasmid using an ECM 830 Electropo (BTX, San Diego, CA, U.S.A.) following the manufactu instructions, then plated on to a collagen type I-coated 35- diameter dish (Iwaki, Chiba, Japan). After 4 h, the medium replaced with DMEM and 10% (v/v) FBS. Cells were harvest 0, 24 and 48 h after transfection. The cell viability was determ with Trypan Blue soon after transfection, and the efficiency estimated by fluorescent microscopy 24 h after transfection the plasmid vector AFP (kindly provided by Dr Hidesato Og Graduate School of Biological Sciences, Nara Institute of Sci and Technology, Japan).

Table 1 Primers for RT-PCR

Name	Direction	Sequence	Product size (bp)	Accessio number
β-Actin	Forward	5′-AAATCGTGCGTGACATCAAA-3′		
	Reverse	5′-AAGGAAGGCTGGAAAAGAGC-3′	178	X03765
Runx3	Forward	5′-GGTTCAACGACCTTCGATTC-3′		
	Reverse	5′-AGGCCTTGGTCTGGTCTTCT-3′	180	NM_019
Runx2	Forward	5′-CAGACCAGCAGCACTCCATA-3′		
	Reverse	5′-CAGCGTCAACACCATCATTC-3′	178	NM_009
Osterix	Forward	5′-GGTCCAGGCAACACACCTAC-3′		
	Reverse	5′-GGTAGGGAGCTGGGTTAAGG-3′	178	AF184
Dspp	Forward	5′-GGAACTGCAGCACAGAATGA-3′		
	Reverse	5′-CAGTGTTCCCCTGTTCGTTT-3′	199	NM_01
Enamelysin	Forward	5′-CGACAATGCTGAGAAGTGGA-3′		
	Reverse	5′-CCCTTTCACATCATCCTTGG-3′	180	NM_01
Klk4	Forward	5′-TTGCAAACGATCTCATGCTC-3′		
	Reverse	5′-TGAGGTGGTACACAGGGTCA-3′	228	NM_01

Real time RT (reverse transcriptase)-PCR analysis

Total RNA was extracted by using Trizol (Invitrogen), and 2 μ freshly isolated RNA was reverse transcribed with SuperScr RT (Invitrogen) following the manufacturer's recommendat The resulting cDNA was then amplified by real time RT- with a Light Cycler-FastStart DNA master SYBR Green I (R Diagnostics, Mannheim, Germany). The primers used in the PCR analysis are presented in Table 1.

Preparation of nuclear extracts

Nuclear extract was isolated as described previously [22]. Br mouse DPCs were washed with 10 ml of PBS, scraped into 1 of ice-cold PBS, and centrifuged at 100 *g* for 5 min. The was suspended in 1 ml of PBS and centrifuged again at

for 15 s. After resuspension in cold buffer A [10 mM Hepes, pH 7.9, 10 mM KCl, 0.1 mM EDTA, 0.1 mM EGTA, 1mM DTT (dithiothreitol) and 0.5 mM PMSF] on ice for 15 min, the cell membranes were lysed by 0.5 % Nonidet P40 and then centrifuged at 660 *g* for 30 s. The pelleted nuclei were resuspended in cold buffer C (20 mM Hepes, pH 7.9, 0.4 M NaCl, 1mM EDTA, 1 mM EGTA, 1 mM DTT and 1 mM PMSF). The nuclear protein was extracted by shaking at 4 °C for 15 min, followed by centrifugation at 15 000 *g* for 5 min and the supernatant fractions were collected. The protein content of the nuclear extracts was determined using the Bradford method [23].

EMSA (electrophoretic mobility-shift assay)

Individual oligonucleotides were annealed to equimolar amounts of their complementary strands (wild-type, Osterix-gel-WT-5′-1: 5′-CAGATCTCTAATTAGTGGTTTGGGGTTTGTTCCT-TTTC-3′ and Osterix-gel-WT-3′-2: 5′-GAAAAGGAACAAAC-CCCAAACCACTAATTAGAGATCTG-3′; mutant, Osterix-gel-MT-5′-1: 5′-CAGATCTCTAATTATAGACTTGGGGTTTGTTC-CTTTTC-3′ and Osterix-gel-MT-3′-2: 5′-GAAAAGGAACAA-ACCCCAAGTCTATAATTAGAGATCTG-3′) by heating to 95 °C for 5 min and cooling slowly to room temperature (25 °C). DIG (digoxigenin) Gel Shift Kit, 2nd generation (Roche Diagnostics) was used in the EMSA according to the manufacturer's protocol. Briefly, wild-type double-stranded oligonucleotide probes were labelled with DIG-11-ddUTP at the 3′-ends. The labelled probes (20 fmol) were added to 10 μg of nuclear extract in a binding buffer [20 mM Hepes, pH 7.6, 1 mM EDTA, 10 mM $(NH_4)_2SO_4$, 1 mM DTT, 0.2 % (w/v) Tween 20, 30 mM KCl, 25 ng/μl poly(dI-dC) · (dI-dC), 25 ng/μl poly(dA-dT) · (dA-dT) and 50 ng/μl poly L-lysine] at room temperature for 30 min. For competition experiments, 125-fold unlabelled oligonucleotides were added to the mixture. After incubation, the protein–DNA complexes were separated by native PAGE (6 % gels), transferred on to a nylon membrane (Whatman, New Jersey, NJ, U.S.A.) by contact-blotting, and detected by the DIG-detection kit. An anti-Runx3 antibody (Active Motif, Carlsbad, CA, U.S.A.) was used to examine the specificity of the protein–DNA complexes.

ChIP (chromatin immunoprecipitation) assay

Mouse DPCs were treated for 10 min with 1 % formaldehyde and washed three times with ice-cold PBS. The cells were harvested and centrifuged at 100 *g* for 5 min. The pellet was suspended in 200 μl of SDS lysis buffer [50 mM Tris/HCl, pH 8.0, 10 mM EDTA, 1 % (w/v) SDS, 1 mM PMSF, 1 μg/ml aprotinin and 1 μg/ml leupeptin] and incubated on ice for 20 min. The sample was sonicated for 7.5 min (high power, on 30 s, off 1 min) using a Bioruptor (Cosmo Bio, Tokyo, Japan) to produce soluble chromatin with an average size of 500 bp. The chromatin sample was then diluted 9-fold in ice-cold ChIP dilution buffer [50 mM Tris/HCl, pH 8.0, 167 mM NaCl, 1.1 % (v/v) Triton X-100, 0.11 % sodium deoxycholate, 1 mM PMSF, 1 μg/ml aprotinin and 1 μg/ml leupeptin]. From the diluted sample, 200 μl was removed as the input fraction and kept at 4 °C. The rest of the sample was pre-cleared for 6 h at 4 °C by incubation with 60 μl of protein G–Sepharose beads pre-blocked with salmon sperm DNA. The beads were removed by centrifugation at 10 000 *g* for 10 s and the supernatant was collected. Rabbit anti-Runx3 polyclonal antibody (20 μg; Active Motif, Carlsbad, CA, U.S.A.) or 10 μg of goat anti-mouse Runx2 polyclonal antibody (Santa Cruz, CA, U.S.A.) was added and incubated overnight at 4 °C. To collect the immunocomplex, 60 μl of protein G–Sepharose beads pre-blocked with salmon sperm DNA were added to the samples for 3 h at 4 °C. The beads were washed once in each of the following buffers, in order: low salt, high salt and LiCl wash solution, and were then washed twice in TE buffer. The bound protein–DNA immunocomplexes were eluted twice with 200 μl of ChIP direct elution buffer (10 mM Tris/HCl, pH 8.0, 300 mM NaCl, 5 mM EDTA and 0.5 % SDS) and subjected to reverse cross-linking at 65 °C for 6 h. The reverse cross-linked chromatin DNA was further purified by 50 μg/ml proteinase K digestion at 55 °C for 1 h and phenol/chloroform extraction. DNA was then precipitated in ethanol and dissolved in 20 μl of TE buffer. DNA (2 μl) was used for each PCR with primers Osx-ChIP-F: 5′-GAGTGTCG-TCCCCAATCC-3′ and Osx-ChIP-R: 5′-CTGCTACCACCG-AGGCTG-3′, yielding a 120 bp product. As a negative control, another 1×10^7 mouse DPCs was treated as above, except 20 μg rabbit IgG or 10 μg goat IgG antibodies were used instead of specific antibodies. Input (diluted 1:20) was used as the positive control for PCR.

Statistics

Statistical analyses were performed using Student's unpaired *t* test. Each experiment was performed at least twice, and the representative data are presented as means ± S.D. for at least three independent replicates.

RESULTS

Expression of *Runx3*, *Runx2*, *Osterix* and *Bmp2* during tooth development

In the developing tooth, *Runx3* was detected in the dental papillae at the late cap stage (15.0 days post coitum). *Runx3* was progressively restricted to the odontoblastic layer of tooth germ from the bell stage (17.0 days post coitum) until the differentiation stage, P1 during terminal differentiation of odontoblasts (Figures 1A–1D). In contrast, *Osterix* was first detected in the odontoblastic layer at 17.0 days post coitum, and was more pronounced at P1 and P4 (Figures 1E–1H) and had overlapping expression with *Runx3*. In the odontoblasts, *Bmp2* also was strongly expressed at P1 (Figure 1O), but not *Runx2* (Figure 1K). No positive signal was detected when using sense probes.

Expression of *Runx3* and *Osterix* during differentiation of the dental pulp cells into odontoblasts *in vitro*

We next determined whether the mouse DPCs have *in vitro* expression patterns of *Runx3* and *Osterix* similar to those observed *in vivo*. RT-PCR was performed to examine gene expression of *Runx3*, *Osterix* and the odontoblast markers *Dspp* (dentin sialophosphoprotein), *enamelysin* and *KLK4* (kallikrein 4) in cell culture (Figure 2A). *Dspp* and *KLK4* were first detected clearly on day 21 and *enamelysin* on day 28, showing spontaneous differentiation of the DPCs into odontoblasts. *Runx3* expression was weakly detected on day 1, and increased further on day 21. *Osterix* expression was first detected on day 21 (Figure 2A). These results correlated with the *in vivo* expression during tooth development, suggesting that the DPCs might be useful for the study of the regulation of expression of *Osterix* by Runx3 at the stage before terminal differentiation of odontoblasts.

Runx3 down-regulates *Osterix* expression in mouse DPCs

To examine whether *Osterix* expression was regulated by Runx3, MSCV-EGFP-Flag-Runx3 was transfected by electroporation into the mouse DPCs. Electroporation, at three square-wave pulses at a frequency of 1 Hz with a pulse length of 99 μs and 1350 V, provided an optimal method for gene transfer *in vitro*. The cell